Neuromuscular Disorders and Techniques: Novel Observations and Fresh Looks

William Pryse-Phillips, MD, FRCP, FRCPC
Jay P. Shah, MD
Vanda A. Lennon, MD, PhD
Homayoon Kazerooni, PhD
Luca Padua, MD, PhD
Neeraj Kumar, MD

2006 Plenary
AANEM 53rd Annual Meeting
Washington, DC

American Association of Neuromuscular & Electrodiagnostic Medicine
2621 Superior Drive NW
Rochester, MN 55901

Printed by Johnson Printing Company, Inc.

Neuromuscular Disorders and Techniques: Novel Observations and Fresh Looks

Faculty

William Pryse-Phillips, MD, FRCP, FRCPC

Emeritus Professor
Department of Neurology
Memorial University
St. John's, Newfoundland, Canada

Dr. William Pryse-Phillips is an emeritus professor of medicine (neurology) at Memorial University in St. John's, Newfoundland, Canada. After completing medical school at Guy's Hospital in the United Kingdom, he trained in medicine, psychiatry, and neurology in England before emigrating to Canada in 1970, working at Queen's and McGill Universities before his appointment at Memorial in 1972, where he has remained since. Dr. Pryse-Phillips has been a member of the Association since 1982, and served as a member of the AANEM's Education Committee and as a board examiner for the ABEM.His books published over the last 30 years are *Epilepsy*, *Essential Neurology*, and *Companion to Clinical Neurology*. He has published over 110 peer-reviewed journal publications and book chapters dealing with migraine, multiple sclerosis, medical ethics, and genetic conditions including myotonic dystrophy and hereditary neuropathies. His interests outside medicine include extreme gardening, iconoclasm, and writing for pleasure.

Jay P. Shah, MD

Director
Medical Rehabilitation Training Program
National Institutes of Health
Bethesda, Maryland

Dr. Jay Shah is a staff physiatrist and Director of the Medical Rehabilitation Training Program in the Rehabilitation Medicine Department of the Clinical Research Center at the National Institutes of Health (NIH). His interests include the neurobiology and pathophysiology of neuromusculoskeletal pain and the integration of physical medicine techniques with promising complementary approaches in the management of neuromusculoskeletal pain and dysfunction. Dr. Shah has given many invited lectures on mechanisms of chronic pain, myofascial pain, acupuncture techniques, and other related topics. He and his co-investigators at the NIH are utilizing novel microanalytical techniques to study the unique biochemical milieu of myofascial trigger points and recently published their findings in the *Journal of Applied Physiology*. Dr. Shah is also a guest faculty and instructor in the Harvard Medical School "Medical Acupuncture for Physicians' course and the New York Medical College "Certificate for Medical Acupuncture Training" course.

Vanda A. Lennon, MD, PhD

Professor
Departments of Immunology and Neurology
Mayo Clinic
Rochester, Minnesota

Vanda A. Lennon, MD, PhD, is Professor of Immunology and Neurology at Mayo Clinic College of Medicine in Rochester, Minnesota, Director of the Autoimmune Neurology Fellowship Program at Mayo Clinic's Department of Neurology, and Director of the Neuroimmunology Laboratory in the Department of Laboratory Medicine and Pathology. She was born in Sydney, Australia, emigrated to the United States as a National Multiple Sclerosis Society Postdoctoral Fellow in 1972, and became a citizen in 1993. Dr. Lennon joined the Consulting Staff of Mayo Clinic in 1978 as founding Director of the Neuroimmunology Laboratory. Her formal education was in medicine, with postgraduate training in immunology and neuroscience. Her research career has focused on organ-specific autoimmunity as it relates to the nervous system and as a manifestation of tumor immune responses. Her particular interest is in plasma membrane antigens of the nervous system that are targets of pathogenic autoantibodies: cation channels in muscle and neurons and, most recently, the aquaporin-4 water channel protein in astrocytes. In 1999, she received the Doctor of the Year Award from the Myasthenia Gravis Foundation of America.

Homayoon Kazerooni, MD, PhD

Professor
Department of Mechanical Engineering
University of California, Berkeley
Berkeley, California

Dr. Kazerooni holds a doctorate in mechanical engineering from Massachusetts Institute of Technology and is currently a professor in the Mechanical Engineering Department at the University of California, Berkeley. He is also the director of the Berkeley Robotics and Human Engineering Laboratory. Dr. Kazerooni has published over 160 articles on robotics, human machine systems, control sciences, artificial locomotion, assist devices, and mechatronics. As a life-long inventor, he is the holder of fifteen patents. He has designed many machines and systems; two systems are currently marketed worldwide by major material handling manufacturers and one system is being evaluated to be marketed. He has served in a variety of leadership roles in the robotics community. Dr. Kazerooni has served as associate editor of two journals: the *American Society of Mechanical Engineers (ASME) Journal of Dynamics Systems and Control* and *ASME/Institute of Electrical and Electronics Engineers Transaction on Mechatronics*.

Luca Padua, MD, PhD

Professor
Department of Neurosciences
Università Cattolica
Rome, Italy

Dr. Padua holds a medical degree with a specialization in neurology as well as a doctorate in neurosciences. He has been a researcher in the Department of Neuroscience and a professor of clinical neurophysiology at the Università Cattolica, as well as a professor of neurology. Dr. Padua's professional activities include positions as Coordinator of the Italian Carpal Tunnel Syndrome of the Italian Neurological Society, a member of the Advisory Board of the Italian Peripheral Neuropathy Study Group, and Coordinator of the Quality of Life Study Group of the Italian Neurological Society. He also serves as a member of the Editorial Board of the *Journal of Sports Medicine and Physical Fitness*, and a reviewer for *Neurology*, *Muscle & Nerve*, *Neurological Sciences*, and *Clinical Neurophysiology*.

Neeraj Kumar, MD

Assistant Professor
Department of Neurology
Mayo Clinic
Rochester, Minnesota

Dr. Kumar received his medical degree from Maulana Azad Medical College at the University of Delhi. He later performed a residency in internal medicine at East Tennessee State University and a residency in neurology at the University of Minnesota. He then had a fellowship at the University of Minnesota in clinical neurophysiology. Dr. Kumar is board-certified in neurology, internal medicine, and electrodiagnostic medicine. He has received the Distinguished Teaching Award from the Minnesota Medical Foundation and in 2005 was named Teacher of the Year by the Mayo Fellows Association. His current research interests include disorders of copper metabolism and medical education research.

Authors had nothing to disclose.

Program Chair: Benn E. Smith, MD

The ideas and opinions expressed in this publication are solely those of the specific authors and do not necessarily represent those of the AANEM.

Neuromuscular Disorders and Techniques: Novel Observations and Fresh Looks

Contents

OBJECTIVES At the conclusion of the plenary session, participants will be able to: (1) outline the process of taking a clinically suspected inherited neuromuscular disorder from the bedside to the genetics laboratory, (2) describe current models of the physiologic basis for neuromusculoskeletal pain, (3) explain recent novel observations in the pathophysiology of autoimmune neuromuscular disorders, (4) provide examples of mechanical robotic strategies to aid human movement in health and disease, (5) review the current developments in understanding neural conduction responses in cutaneous digital nerves, and (6) summarize the neuromuscular disorders and deficits which may result from copper deficiency.

PREREQUISITE This course is designed as an educational opportunity for residents, fellows, and practicing clinical EDX physicians at an early point in their career, or for more senior EDX practitioners who are seeking a pragmatic review of basic clinical and EDX principles. It is open only to persons with an MD, DO, DVM, DDS, or foreign equivalent degree.

ACCREDITATION STATEMENT The AANEM is accredited by the Accreditation Council for Continuing Medical Education to provide continuing medical education (CME) for physicians.

CME CREDIT The AANEM designates this activity for a maximum of 3.25 hours in *AMA PRA Category 1 Credit(s)*™. This educational event is approved as an Accredited Group Learning Activity under Section 1 of the Framework of Continuing Professional Development (CPD) options for the Maintenance of Certification Program of the Royal College of Physicians and Surgeons of Canada. Each physician should claim only those hours of credit he or she actually spent in the educational activity. **CME for this course is available 10/06 - 10/09.**

2005-2006 PROGRAM COMMITTEE

Benn E. Smith, MD, Chair
Scottsdale, Arizona

Michael T. Andary, MD,MS
East Lansing Michigan

Charles G. Burgar, MD
Temple, Texas

Joseph H. Feinberg, MD
New York, New York

Brent Goodman, MD
Scottsdale, Arizona

Robert Irwin, MD
Miami, Florida

Rajasekhar V. Kandala, MD
Long Beech, California

Robert N. Kurtzke, MD
Fairfax, Virginia

William J. Litchy, MD
Rochester, Minnesota

Christina M. Marciniak, MD
Chicago, Illinois

Zachary Simmons, MD
Hershey, Pennsylvania

Jeffrey A. Strommen, MD
Rochester, Minnesota

Steven Vernino, MD, PhD
Dallas, Texas

2005-2006 AANEM PRESIDENT

Janice M. Massey, MD
Durham, North Carolina

The Agony of Analgesia: Hereditary Sensory Neuropathies in Newfoundland

William Pryse-Phillips, MD, FRCP, FRCPC

Emeritus Professor of Medicine (Neurology)
Memorial University of Newfoundland
St. John's, Newfoundland, Canada

INTRODUCTION

Dr. William Harvey once presented a case to the English King Charles I:

> *2 December 1633. Lord Northumberland...heard Dr. Harvey tell the King that he had been to see a homan (sic) in St. Thomas' Hospitall in Southwark who had no feeling at all, that he burnt her Neck and Cheeke with a hot yron; and that she being in bed, he put in his hand and pulled of some hayre of her pryvy partes and she never felt any thing or seemed not to feele . . . That she tooke a pot, and could gripe it in her hand and hold it, but unless she saw it she knew not whether she held it or no. That if her Hand and Arme were wrung she found a little pressure but no paine at alle, nor any sense in the skin or outward partes, but as if there were twenty paires of gloves between her and that which touched her.*

What was this condition? The brief description suggests that there was trunkal involvement, loss of touch as well as pain, but somewhat retained pressure sensation and apparently intact motor power. Without pain or common touch sensation in the face, limbs, and trunk in the presence of normal motor power in the hands, either central or peripheral pathologies might be suspected, but from this description one can achieve neither localization nor a confident diagnosis.

In 1846 the French physician Leplat described *mal perforant du pied* (foot ulcers), almost certainly indicating a peripheral sensory neuropathy. Six years later, Nélaton reported similar cases with three of six adult brothers affected, and in 1883, Morvan described similar patients from Brittany. In Movan's reported cases, the problem was not inherited and the onset arose in middle life; syringomyelia was diagnosed. Sir Henry Head of England, presented a case in 1900 of an areflexic child of 3 years with total pain loss. Post-mortem data were not published for any of these patients and the site of their lesions remains now, as then, problematic.

In 1921, the District Medical Officer working on the north-east Newfoundland coast reported on a family living in that area of the island:

> *"Mr. J. L. of Loon Bay in Lewisporte, born about 1880, lost the most extreme parts of feet and fingers...through, as I recall from my only sight of him about 1921, being caught out in a snowstorm and having them frostbitten, from which there set in... a process of creeping receding gangrene in the course of which other toes and fingers became infected from their neighbors.*
>
> *"He was about 40 when I saw him at Port Union, T.B. [Trinity Bay] where he had come from Loon Bay to canvass for financial support and was a man with a much wrinkled forehead and a coal black moustache and hair, and in direct answer to my question as to who had done the successive amputations he described to me as having been performed as the disease receded, he told me he had done most of them himself."*

In both of these patients, the major finding was an impairment of the appreciation of pain. Theoretically, this could be due to a central, likely cortical problem (some kind of central processor), or to a lesion in the peripheral nervous system (PNS) (the pathway). If is unfortunate that the terminology used is so confusing. This author suggests that the problem may lie either in the brain or in the peripheral nerves and that the phenotypes differ enough to allow clinical differentiation (Table 1).

ANALGESIA OF CENTRAL ORIGIN (PAIN INDIFFERENCE OR ASYMBOLIA)

In analgesia of central origin there is a physiological perception of a sensation, but it lacks any affective (painful) quality. Examples from the literature and the press include the case of Mr. Edward Gibson (The Human Pincushion) whose repetitively staged crucifixions caused so many in his 19th century audiences to swoon that his demonstrations were forbidden. Contemporary psychiatric diagnoses of the same entity included hysteria, sado-masochism, and psychotic depression.

Features suggesting the presence of a central lesion include the association of other central nervous system (CNS) abnormalities, the co-occurrence of behavioral disturbances such as self-mutilation, the fact that there are few or no PNS abnormalities clinically, and that nerve biopsies have been reported as normal. Features against a central lesion are that some PNS abnormalities have been reported, that postmortem results are sparse or missing, and that modern methods were not employed in nerve biopsy studies.[12]

ANALGESIA OF PERIPHERAL ORIGIN (PAIN INSENSITIVITY OR IMPERCEPTION)

Many other syndromes present with loss of pain sensitivity and enter into the theoretical differential diagnosis.

Acquired conditions include alcoholic neuropathy, diabetic pure sensory (thin fiber type) neuropathy, leprosy, and beriberi. Beriberi was a common diagnosis in Newfoundland patients early in the 20th century.

Genetic conditions include analphalipoproteinemia (Tangier disease) abetalipoproteinemia (Bassen-Kornzweig disease), Fabry disease, giant axonal neuropathy, and familial amyloid (Type 1, Andrade's syndrome), all of which have known biochemical bases. The remaining inherited disorders are mainly hereditary sensory and autonomic neuropathies (HSANs) in Dyck's terminology (Table 2).[2] The first definitive reports of HSAN 1 and 2 were by

Table 1 Some Conditions Leading to Unawareness of Pain

1. Faults in the Processor		
Dissociated mental states; hysteria, hypnosis, religiose ecstasy, and other profound emotional experiences as in battle and sport		
Mental retardation (?)		
Frontal lobotomy (sensation retained, suffering diminished)		
Parietal lobe lesions		
Post-encephalitic		
Congenital indifference to pain (asymbolia)		
2. Faults in the Pathway		
Without Defined Biochemistry/Morphology		
Hereditary sensory/autonomic neuropathies (HSAN) 1 - 5		
Hereditary motor and sensory neuropathies (HMSN) (some)		
With Defined Biochemistry/Morphology		
HMSN 4 (Refsum)	Bassen-Kornzweig	Tangier disease
Fabry disease	Lesch-Nyhan syndrome	Amyloid neuropathies
Giant axonal neuropathy		
Acquired		
Acute pandysautonomia	Rheumatoid	Diabetic neuropathy (small-fiber type)
Leprosy Alcohol/Beriberi	Paraneoplastic	
(Tabes dorsalis)	(Syringomyelia)	

Table 2 Major Genetic Neuropathies Without Known Biochemical Bases

Dominant	Recessive	X-Linked
HMSN 1	HMSN 3 (D-S)	HSAN
HMSN 2	HMSN 4 (Refsum)	
HMSN 5	HMSN 6	
HSAN 1	HSAN 2	
+ paraplegia	+ paraplegia	
	+ neurotrophic keratitis	
	HSAN 3 (dysautonomia)	
	HSAN 4 (pain insensitivity + dysautonomia + central lesion)	
	?HSAN 5	

HMSN = hereditary motor and sensory neuropathy; HSAN= hereditary sensory autonomic neuropathy

Denny-Brown[1] and Orgyzlo[7] respectively. Many of the original patients of Orgyzlo are still living in Newfoundland, and it was these kinships that this author has been able to study since 1972.

FAMILY STUDY OF HEREDITARY SENSORY AUTONOMIC NEUROPATHY IN NEWFOUNDLAND

The island of Newfoundland has a 6000 mile coastline, but all the patients studied were descended from the original immigrant family members who came to Newfoundland from Dorset or Devon (in southern England) in the early 1800s and who have settled a 100 mile stretch of the northeastern coast over the last 200 years. While some of their descendants continue to inhabit the same outports and towns, others have moved within the island or to the mainland of Canada. There is no known French connection, although genetically identical cases have been found in Quebec.

This author found at least 64 affected subjects in 4 kinships. While a few subjects had the clinical features typical of HSAN 2, far more manifested the HSAN 1 phenotype and the two conditions required careful clinical differentiation for genetic analysis to succeed. The study initially comprised clinic and home visits and community screening. Later, colleagues in the Genetics Discipline of Memorial University and staff at Xenon, Inc., Vancouver, BC collaborated respectively to refine the family trees and to perform genetic linkage analyses.

CLINICAL FINDINGS IN THE NEWFOUNDLAND CASES

Hereditary sensory autonomic neuropathy type 2 was first noted in Newfoundland in the early 1900s. The original family members came from Dorset, United Kingdom, 100 years earlier, as part of a mass westerly migration of settlers from southwestern England and southern Ireland.[10]

Beginning in early childhood, the affected individuals examined in this study experienced numbness in their hands and feet, aggravated by cold, together with reduced sensation to pain (Table 3). They experienced loss of touch, pain, and temperature, with touch being most severely affected. The loss was predominantly distal, extending gradually from the fingertips to the elbows, and from the toes to the thighs in a typical "glove and stocking" distribution. The legs were affected earlier and more severely than the arms. Progression of the disorder varied within the family, but in the most affected subjects there was sensory loss over the manubrium and the vertex of the scalp. Muscle atrophy was occasionally noted, but diminished muscle stretch reflexes, ulcerations, and infections were

Table 3 Summarized Clinical Features of the Newfoundland HSAN 2 Kinships

Onset age/ First symptoms	Congenital / 4-8 years
Mutilating acropathy	Common
Self-mutilation	Not recorded
Lancinating pains	Uncommon
Modes affected	All; but mainly skin and deep pain, temperature and touch
Distribution	Toes, feet & legs > fingers, hands and arms
Motor involvement	Overt signs rare
Muscle stretch reflexes	Absent or much diminished
Sensory potentials	Absent
MNCVs	Normal or slightly slowed
Nerve pathology	Demyelination, all fiber sizes

HSAN= hereditary sensory autonomic neuropathy; MNCVs = motor nerve conduction velocities

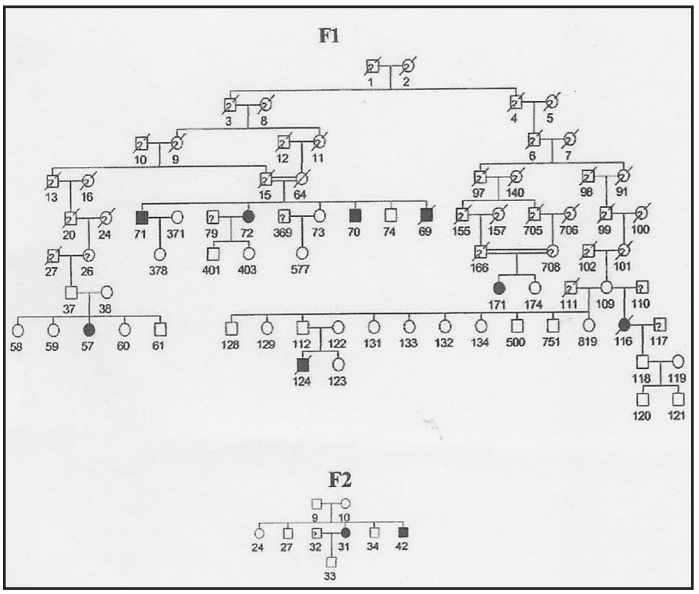

Figure 1 Family trees of two Newfoundland HSAN 2 kinships. The pseudo-dominant pattern of transmission of the disease can be ascribed to the first- and second-cousin marriages shown; autosomal recessive inheritance provides the best explanation (from Lafrenière and colleagues[4] with permission).

CSF = cerebral spinal fluid; HSAN= hereditary sensory autonomic neuropathy

common and caused spontaneous amputation of digits and surgical amputation of lower limbs.

Autonomic dysfunction was only seen in the impairment of skin circulation. Mental development, sweating, and tearing were normal and postural hypotension was not found. As in other HSANs there was absence of axon flare after dermal scratch, indicative of defective nociceptive fibers. Biopsy revealed a severe loss of myelinated axons, some loss of nonmyelinated fibers in the sural nerve, and the absence of cutaneous sensory receptors and nerve fibers.

The clinical effects could be devastating, unnoticed traumata leading on to ulcerations, infection, osteomyelitis and successively more proximal amputations. In one case, a teenager complained to his mother one evening that he could not get his sneaker off his foot. The cause was found to be a 3-inch nail that had perforated the sneaker sole, piercing the foot and nailing it within the shoe, unbeknownst to the boy. In patients from older generations, their bilateral leg and upper limb digital amputations produced a picture resembling phocomelia.

Most amputations have been performed during the second (feet, legs) or the third decade (fingers). Further amputations have been unusual since the existence of the condition has been made known to parents in the kinship, who have also been taught to make careful daily inspection of their childrens' feet; and to ensure that only safe, strong, footwear and gloves are worn.

Although most patients were aware of impaired sensation in their feet for as long as they can remember, similar sensory impairment

Table 4 Usual Features of Hereditary Sensory & Autonomic Neuropathies 1 & 2*

	HSAN 1	HSAN 2
Inheritance recessive	Autosomal dominant	Autosomal
Variability	Extreme	Minor
Clinical onset	10-50 years	Congenital-10 years
Acropathy	Feet	Hands and feet
Course progression	Slowly progressive	Static/slow
Lancinations	Yes	Seldom
Modes affected	Pain, Temp > others	All modes
Areas affected	Distal	Limbs and trunk
Motor signs	Common	Uncommon
Reflexes	Diminished or lost	Diminished or lost
Autonomic signs	Present if sought	Present if sought
Associations	OPCA, Friedreich disease pes cavus, HMSN VII palsy, pyramidal signs Deafness	Uncommon
MNCV	Normal/slight slowing	Normal
SNAPs	Absent	Absent
Biochemistry	Increased serum IgA levels	
Pathology	Dec. A & C fibres, especially distally = dying back. Myelin damage secondary	Myelinated fiber loss especially distally = dying back. Dec. TV fascicular area and # of unmyelinated fibers. Degenerating fibres
Plasmapheresis	Improvement, 1 case	Unreported

(Composite from Pryse-Phillips;[9] Dyck;[2] Nagasako;[6] Scott[11])

MNCV = motor nerve conduction velocity; SNAPs = sensory nerve action potential; OPCA = olivopontocellar atrophy; HMSN = hereditary motor and sensory neuropathy; Dec. TV = decending ??

in the fingers and hands was seldom noticed before the age of 10 years. Thereafter, progression was slow and in all cases the face was spared, except for small patches of impairment of skin pain and of light touch in one or two subjects. This author's patients with HSAN 2 have shown slow progression for the first 25-30 years of life, after which time the condition stabilized and the rate of further loss of sensation slowed almost to a standstill—although there was less left to lose by that time. Therefore, this is probably not a neural crest lesion, but rather a metabolic disease with ongoing effects upon some part of the peripheral sensory neurons.

The clinical picture did not accord with any of the many variant forms of HSAN described, such as HSAN with abnormal amino-acids in the CSF; HSAN 2 (like) with dysautonomia and corneal insensitivity; HSAN 2I; HSAN 4; HSAN 5; HSAN and tonic pupil; axelrod sensory neuropathy; X-linked HSAN.[2,6,9]

GENETIC STUDY

A whole genome scan was performed using 800 markers (~5 cm).[4] There was no perfect homozygous allele sharing in the seven affected subjects, indicating presumptive recombination. Pair-wise linkage analysis was then performed using MLINK from the FASTLINK v4.1p program, allowing for known pedigree consanguinity loops and assuming equal allele frequencies. Eight chromosomal regions with sum LOD > 2.0 were found on chromosome 12p (LOD 2.64 at q = 0). Using GENEHUNTER v2.1_r2 beta haplotypes were constructed on pedigree sections, which were manually combined. As a result, a novel gene was identified mapping within intron 8 of the PRKWNK1 gene.

CENTRAL AND PERIPHERAL ANALGESIC STATES

Thrush[12] suggested the following criteria for the diagnosis of analgesia of central origin (congenital insensitivity to pain)

The whole body should be affected.

The condition should be congenital and nonprogressive.

No other modality should be affected.

Itch and tickle sensations were normal in his cases, but corneal reflexes were absent, as in most other cases to date. He concluded that a central lesion in the dorsal horn or in the RAS was the most likely cause and reviewed the various cortical features associated, including anosmia, ageusia, hyperhidrosis, and parasympathetic abnormalities (tears, pupils, esophagus). His nerve biopsies showed that many unmyelinated fibers were present, but there was an absence of large myelinated fibers with some evidence of regeneration.

The phenomenon of pain insensitivity has been reviewed by Nagasako and colleagues[6] who highlighted the terminological confusion surrounding the subject (various names and definitions used without clear distinction as to etiology or pathophysiology). For example, they refer to a definition of congenital indifference to pain as a condition in which pain is perceived, but does not hurt. This does not clarify the definition of pain. They also show that there are three terms in current usage with significant overlap in meaning. The first is congenital insensitivity to pain which is used for some peripheral neuropathies with reduction or loss of pain appreciation. The second is congenital indifference to pain or congenital universal insensitivity to pain, in which there is pure pain loss, all other sensations being normal, and in which the peripheral nerve morphology may or may not be abnormal. The term is a misnomer because one can hardly react to a sensation that one is not capable of appreciating. The third is asymbolia, where central processing of pain is impaired as a result of lesions of the cingulate, insular, or somatosensory cortices.

The distinction between the last two of these appears to be dependent on finding (or perhaps looking for) a cerebral lesion. This author suggests that the use of these terms is confusing and redundant, and that in this context, analgesic states should be classified simply as having a central or a peripheral pathology; analgesia of peripheral origin (APO) such as HSANs 1 and 2 versus analgesia of central origin (ACO), such as asymbolia. Thus it seems logical to suppose that there are four possibilities that comprehend the nature of the underlying problems:

Table 5 Features of Analgesia of Peripheral Origin (HSAN 1 and 2) Versus Analgesia of Central Origin (Congenital Indifference to Pain, Asymbolia)

	APO	ACO	
Self mutilation	Rare		Common
CNS signs	Rare		Cortical, if sought
Motor involvement	HSAN 1		None
Fiber loss	All + ANS	None	
Distribution	Peripheral, centripetal		Universal
Course	Slow progression		Static
Onset Congenital	< 10 years		
Sensory modes deficient	All; pain > others		Pain only
Spontaneous pains	Common		Absent

ACO = analgesia of central origin; ANS = autonomic nervous system; APO = analgesia of peripheral origin; CNS = central nervous system; HSAN= hereditary sensory autonomic neuropathy

First, there may be a central lesion leading to the clinical features defined by Thrush.[12] In such cases, loss of pain sensation is the sole sensory manifestation with touch and other sensory modes being retained. Other CNS features may be present. These may be defined as ACO. Second, there may be central lesions that lead to the loss of various sensations, including pain. Numerous structural and other pathologies may be responsible, e.g., tabes dorsalis, cortical lesions, syringomyelia, etc. Third are neuropathies with pure involvement of the A delta and C fibers leading to loss of pain and (usually) of other thin-fiber functions such as temperature sensation, tickle, and itch. Such conditions include some HSANs and are best regarded as examples of APO. Fourth are neuropathies with involvement of a wider spectrum of fibers, as shown by loss of modalities other that of pain, temperature etc. While they are also examples of APO, their associated features should allow them to be differentiated from most of the HSANs (Table 1).

One can conclude that congenital indifference to pain and asymbolia represent a single (likely cortical) condition affecting the operation of some central processor while the different features of the HSANs and other neuropathies, as tabulated above, should allow their clinical differentiation as peripheral problems.

Do motor features allow distinction between hereditary sensory autonomic neuropathy 1 and hereditary sensory autonomic neuropathy 2?

In some of the Newfoundland HSAN 1 kinships, there are significant motor features—so much so that one patient (who willfully denied any family history) was treated with plasma exchange in another Canadian province following the incorrect diagnosis of chromic inflammatory demyelinating polyneuropathy. He experienced notable symptomatic relief.

Denny-Brown1 described the features of HSAN 1 in his index cases and, later, with England[3] questioned whether some of their patients had HMSNs with unusually marked sensory symptoms or HSANs with unusual motor features. Murray[5] described two siblings with congenital sensory neuropathy (HSAN 2) manifesting early onset loss of touch-pressure sensation while some pain sense was retained. Muscle stretch reflexes were lost and there was some evidence of a lower motor neuron lesion. A literature survey revealed reports of subjects with HSAN 1 showing motor involvement in 15 instances out of 20 retrieved, while reports of HSAN 2 with motor signs numbered only 3 among 14 reports.

In this author's HSAN 2 kinship there were minimal motor signs, although in one or two cases there was electromyographic evidence of mild, chronic denervation. Within the HSAN 1 kinships studied, however, motor features were frequently marked. One must conclude that motor signs are suggestive of, though not definitive for, HSAN 1.

GENETIC IDENTIFICATION

Isolation of the responsible gene is a first step in genetic identification, but in order to change the course of the disease in affected subjects, it is necessary to determine what the gene does. The functional domain of the gene is not yet clear; it could be a signal peptide, a secreted factor like nerve growth factor, a developmental regulator, or a substance responsible for neuronal maintenance.[4] One speculative hypothesis as to why a system functions well for some years and then fails would be that there is here the excess formation of a toxic gene product leading slowly to cell death, bearing in mind that in one single, anecdotal case of HSAN 1 (but not HSAN 2), plasmapheresis led to documented as well as subjective improvement.

DOES THE COURSE OF THE DISORDER ASSIST IN UNDERSTANDING PATHOGENESIS?

Dyck[2] questioned whether HSAN 2 is a static or a progressive condition. If static, this would suggest that a developmental failure such as a disorder of differentiation of the neural crest could be the fault, but if progressive, a metabolic disorder, impairing the metabolism of the sensory ganglion cell and its axon, would be more likely, but unequivocal evidence of progression has not hitherto been brought forward. In the kinships studied by the author, the course was slowly progressive up to the point of involvement of the whole of each limb and distal trunkal and cranial regions (manubrium and vertex).

CONCLUSIONS

Hereditary sensory autonomic neuropathies are among the causes of APO, while the condition known as congenital indifference to pain, or asymbolia, represents ACO. It may be either inherited or acquired and its clinical manifestations differ from those of APO. The term 'insensitivity to pain' is best discarded. Hereditary sensory autonomic neuropathies 1 and 2 manifest decelerating clinical progression. The presence of motor signs, later onset, dominant inheritance, the preferential involvement of pain and temperature sensory modes, the infrequent involvement of the hands and the severity of the lancinating pains all favor the diagnosis of HSAN 1 as opposed to HSAN 2. Early detection of HSANs is possible through careful examination of children at risk, and preventative foot and hand care may prevent amputations. Genetic analysis remains dependent on

clinical capacity. Identification of the gene is but an early step in the search for prevention or for a cure.

References

1. Denny-Brown D. Hereditary sensory radicular neuropathy. J Neurol Neurosurg Psychiatry 1951;14:237-252.
2. Dyck PJ, Chance P, Lebo R, Carney JA. Neuronal atrophy and degeneration predominantly affecting peripheral sensory and autonomic neurons. In: Dyck PJ, Thomas PK, editors. Peripheral neuropathy, volume 2, 3rd edition. Philadelphia: WB Saunders; 1993. p 1065-1093.
3. England AC, Denny-Brown D. Severe sensory changes and trophic disorder, in peroneal muscular atrophy (Charcot-Marie-Tooth type). AMA Arch Neurol Psychiatry 1952;67:1-22.
4. Lafrenière RG, MacDonald ML, Dube MP, MacFarlane J, O'Driscoll M, Brais B, Meilleur S, Brinkman RR, Dadivas O, Pape T, Platon C, Radomski C, Risler J, Thompson J, Guerra-Escobio AM, Davar G, Breakefield XO, Pimstone SN, Green R, Pryse-Phillips W, Goldberg YP, Younghusband HB, Hayden MR, Sherrington R, Rouleau GA, Samuels ME; Study of Canadian Genetic Isolates. Identification of a novel gene (HSN2) causing hereditary sensory and autonomic neuropathy type 2 through the Study of Canadian Genetic Isolates. Am J Hum Genet 2004;74:1064-1073.
5. Murray TJ. Congenital sensory neuropathy. Brain 1973;96:387-394.
6. Nagasako EM, Oaklander AL, Dworkin RH. Congenital insensitivity to pain: an update. Pain 2003;101:213-219.
7. Ogryzlo M. A familial peripheral neuropathy of unknown etiology, resembling Morvan's disease. Can Med Assoc J 1946;54:547-553.
8. Ota M, Ellefson RD, Lambert EH, Dyck PJ. Hereditary sensory neuropathy, type II. Clinical, electrophysiologic, histologic, and biochemical studies of a Quebec kinship. Arch Neurol 1973;29:23-37.
9. Pryse-Phillips W. Companion to clinical neurology, 2nd edition. New York: Oxford University Press; 2003.
10. Rahman P, Jones A, Curtis J, Bartlett S, Peddle L, Fernandez BA, Freimer NB. The Newfoundland population: a unique resource for genetic investigation of complex diseases. Hum Mol Genet Spec 2003;12:R167-R172.
11. Scott KR, Kothari MJ. Hereditary neuropathies. Semin Neurol 2005;25:174-184.
12. Thrush DC. Congenital insensitivity to pain. A clinical, genetic and neurophysiological study of four children from the same family. Brain 1973;96:369-386.

New Frontiers in the Pathophysiology of Neuromusculoskeletal Pain

Jay P. Shah, MD

Staff Physiatrist
Rehabilitation Medicine Department
National Institutes of Health
Bethesda, Maryland

INTRODUCTION

Chronic pain syndromes (e.g., fibromyalgia, myofascial pain syndrome, etc.) exhibit profound neuroplastic changes in neuronal excitability and architecture in the pain matrix (e.g., in the spinal cord, thalamic nuclei, cortical areas, amygdale, and periaqueductal gray). This dynamic process can fundamentally alter one's pain threshold, pain intensity, and affect.

Signaling in the pain matrix may begin with activation of polymodal nociceptors, structures which can also be sensitized by substances released by damaged tissue and the nociceptor terminals themselves. Prolonged noxious input may lead to long-term changes in gene expression, somatosensory processing, and synaptic structure. For example, a continuous barrage of noxious input into the dorsal horn (a process termed "afferent drive") results in the co-release of L-glutamate and substance P. Released together, these two substances can lower thresholds for synaptic activation and open previously ineffective synaptic connections in wide dynamic range (WDR) neurons and cause central sensitization. Sensitization causes upregulation of expression of ion channels and receptors on nociceptors and dorsal horn neurons. Under normal circumstances, a dynamic balance exists between pain facilitating and inhibiting functions. Neurons conveying nociceptive information are controlled by a variety of inhibitory interneurons—structures critically involved in preventing the transition from acute to chronic pain.

Musculoskeletal (MSK) pain is the most common manifestation of chronic pain. Use of the term neuromusculoskeletal pain is preferable as it accurately suggests that the nervous system is fundamentally altered—sometimes irreversibly. The most common type of MSK pain is myofascial pain, or pain that arises from discrete hyperirritable palpable nodules in taut bands of muscle. This form of MSK pain can only be diagnosed by palpation of the soft tissue by an experienced examiner following a thorough medical history. Dry needling or "trigger point acupuncture" is an effective treatment technique. In clinical studies, it has been found to be as effective as lidocaine injection in inactivating a myofascial trigger point (MTrP) and providing symptomatic relief.[1]

The author's preference is to use a 32-gauge acupuncture needle for dry needling MTrPs. An acupuncture needle has a rounded tip compared to the beveled edge of a hypodermic needle and is therefore less painful and less traumatic to tissue. Furthermore, it affords the clinician superior proprioceptive feedback that is helpful in guiding the needle toward the active MTrPs, which are often firm and initially resistant to needle passage.

Because the precise location of the MTrP during injection or dry needling is more important than the anesthetic solution being injected, the local twitch response is a valuable indicator that confirms the accurate location of the MTrP. It is essential to obtain local twitch responses while needling to obtain the desired effect. There is evidence that needling MTrPs in one muscle group may eliminate MTrPs in muscles that belong to the referred pain area of the treated MTrPs.[1] Invasive techniques are not without risk and require thorough knowledge of anatomy, indications, and contraindications.[3,6]

Melzack theorizes that classic acupuncture and trigger point stimulation techniques are generally painful and that they produce analgesia based on overstimulation of the peripheral nociceptive system, inducing a self-regulating pain modulating effect.

He went on to speculate:

> *"…the close correlations between trigger points and acupuncture points for pain is remarkable since the distribution of both types of points are historically derived from such different concepts of medicine. Trigger points are firmly anchored in the anatomy of the neural and muscular systems, while acupuncture points are associated with an ancient conceptual but anatomically non-existent system of meridians which carry Yin (spirits) and Yang (blood). Despite the different origins, however, it is reasonable to assume that acupuncture points for pain relief, like trigger points are derived from the same kind of empirical observation: that pressure at certain points is associated with particular pain patterns, and brief, intense stimulation of the points by needling sometimes produces prolonged relief of pain. These considerations suggest a hypothesis; that trigger points and acupuncture points for pain, though discovered independently and labeled differently, represent the same phenomenon"*[4]

Melzack noted a 71% correspondence between acupuncture points and Travell and Simons' MTrPs in terms of spatial location and referral patterns.[4,8] For example, the referral pattern of a common MTrP in the latissimus dorsi muscle tracks very closely together with the paired heart-small intestine meridian described in traditional Chinese medicine. Perhaps, then, acupuncture meridians and Travell and Simons grid of MTrP's actually represent a guide of where to begin looking for "active" acupuncture points. An overview of the unique neurobiology of muscle pain is needed to better understand this relationship.

THE UNIQUE NEUROBIOLOGY OF MUSCLE PAIN

Muscle pain has several unique characteristics when compared to cutaneous pain: it causes aching, cramping pain, difficult to localize and referred to deep somatic tissues; muscle pain activates unique cortical structures; muscle pain is inhibited more strongly by descending pain-modulating pathways; and activation of muscle nociceptors is much more effective at inducing neuroplastic changes in dorsal horn neurons

SENSITIZATION/ACTIVATION OF MUSCLE NOCICEPTORS

A noxious stimulus acting on a muscle nociceptor (NC) has two options of exciting the nociceptor—deforming the axonal membrane of the ending to threshold or, of clinically higher interest—it can release sensitizing or pain producing substances from the muscle tissue. Bradykinin (BK), prostaglandins (PG) and serotonin (5-HT) are effective at sensitizing muscle nociceptors. A sensitized muscle NC lowers its normally high stimulation threshold into the innocuous range such that it will respond to innocuous everyday stimuli like weak pressure and muscle movement.[5] Furthermore, at sufficient concentrations, BK and 5-HT can directly activate muscle NCs.

Another important point is that the NC endings contain stored substances, e.g., substance P (SP) and calcitonin gene-related peptide (CGRP) that produce vasodilation and plasma extravasation around the NC. Whenever the NC is activated by a noxious stimulus, it releases these substances which directly influence the local microcirculation. Therefore, the muscle NC is not merely a passive receptor that does nothing else but record potentially noxious stimuli. It plays an active role in injured tissue by releasing SP and CGRP which can influence the blood vessels in its vicinity. The sensitization of muscle nociceptors causes the exquisite tenderness when firm pressure is applied over a myofascial trigger point (MTrP).[5]

In contrast to earlier beliefs, the sensitization of a nociceptive ending is not due to nonspecific damage of the ending by a strong stimulus. Rather, it is due to the binding of specific substances (e.g., BK, PG, 5-HT, etc.) to their paired receptors on muscle nociceptors.[5] These receptors are dynamic structures. For example, the BK receptor changes when the tissue is pathologically altered—ordinarily, BK binds to the B2 receptor, but a different BK receptor (B1) is synthesized when the tissue becomes inflamed.

This is an example of neuroplasticity, a process believed to herald the transition from acute to chronic pain. The degree to which MTrP nociceptors become sensitized or activated varies according to how they are stimulated. For this reason, an MTrP may be either in an active pain-producing phase or in a latent non-pain-producing phase.

CENTRAL SENSITIZATION

Myofascial trigger points may not only cause pain and dysfunction, but a chronic MTrP may be a nidus of on-going noxious input that sensitizes dorsal horn neurons, a process that can lead to neuropathic pain. A review of basic muscle pain neurophysiology is helpful in understanding how central sensitization develops.

The primary peripheral sensing apparatus in muscle involves the group III (thinly myelinated low-threshold fibers, identical to Adelta fibers in the skin), and group IV (unmyelinated high-threshold fibers, identical to C fibers in the skin) afferent nerve fibers. These fibers cause aching, cramping pain when stimulated with microneural techniques.

There are important characteristics of the central projections of these fibers including: reduced spatial resolution due to a lower innervation density of muscle tissue compared to the skin, thus making it more difficult to localize muscle pain; convergence of sensory input from skin, muscle, periosteum, bone, and viscera into the same area of the dorsal horn, making it difficult to distinguish the origin of the pain compared to the skin; and divergence of sensory input into the dorsal horn with sustained noxious input leads to the opening of previously ineffective connections (this is especially true of group IV fibers in animal models, which then begin to lower levels of stimulation [mechanical allodynia]).[5]

Compared to normal muscle and muscle with latent MTrPs, muscle with active MTrPs is more tender and mechanically sensitive, suggesting that peripheral nociceptors are already sensitized. Once sensitized, the group IV afferents will fire at lower thresholds, even though they are normally high-threshold nociceptors. For example, an increase in sympathetic input or injection of bradykinin or prostaglandins into the muscle near the active MTrP will cause the group IV afferents to respond to much lower levels of stimulation (i.e., they become sensitized). This phenomenon is believed to contribute to the unusual referral patterns that are seen in myofascial pain syndrome (MPS). For example, active MTrPs in the suboccipital muscles may refer pain to the frontal region and active MTrPs in the piriformis may refer pain in a sciatic nerve distribution.

A nociceptive input from skeletal muscle is much more effective at inducing neuroplastic changes in the spinal cord than is input from the skin.[9] Experimentally induced myositis in animal models causes a marked expansion of the muscle's target area in the dorsal horn. For example, Hoheisel and colleagues found that noxious input from the gastrocsoleus (L5) muscle also activated neurons in the segment L3 which are ordinarily not activated. This is a result of a central sensitization—i.e., the continuous nociceptive input from the L5 muscle made the L3 dorsal horn neurons in the marginal area hyperexcitable, such that they now respond to an input from the muscle that they previously did not.[2]

Moreover, this expansion of the myositis-induced excitation in the spinal cord has clinical relevance because it can explain the spread of muscle pain many patients experience. It also can explain the hyperalgesia many patients report because many of these neurons are hyperexcitable. How do these myositis-induced changes in the spinal cord occur? These changes have been termed "rewiring" because the nociceptive information in the spinal cord takes a completely different course when there is a lesion or noxious input from the muscle (i.e, an MTrP).

SYNAPTIC CONNECTIONS IN THE DORSAL HORN

There are at least two functional types of synaptic connections in the dorsal horn. One is an effective synapse—action potentials arriving at the presynaptic portion of an effective synapse exert a very strong influence on the postsynaptic neuron. The other is a much larger number of ineffective synapses—ineffective because they don't influence the post-synaptic neuron in a way that it fires or is strongly influenced by the noxious afferent input. However, ongoing noxious input from a myositis lesion causes SP to be released from the dorsal root ganglion and to travel into the dorsal horn. Substance P is well-known for its ability to increase the efficacy of synaptic connections in the spinal cord. AP's can then excite neurons in the L3 segment.[2]

Under normal circumstances glutamate is the presynaptic transmitter for nociceptive information in dorsal horn neurons. At the postsynaptic site sit the N-methyl-d-asparate (NMDA) and alpha-amino-3-hydroxy-5-methy-4-isoxazolproprioonic acid (AMPA) receptors for glutamate and the neurokinin receptor 1 (NK1) receptor for SP. A third substance, often ignored, is nitric oxide, which is synthesized from arginine in a small fraction of neurons in the spinal cord; it differs from all known neurotransmitters by its ability to diffuse through all biological membranes.

What are the molecular mechanisms underlying the transition from an ineffective synapse to an effective one? Under normal conditions, only the AMPA channel is active—therefore, if there is impact to a muscle, a short train of impulses causes the presynaptic site to release glutamate, causing a brief activation of the AMPA receptor and postsynaptic neuron. The channel then returns to its resting state. An ineffective synapse does not have AMPA channels. Under normal conditions, only glutamate is released and neurons with ineffective synapses do not respond to a brief nociceptive input, such as a blow to a muscle. However, a strong or prolonged noxious input causes glutamate and SP to be released together. This process can open up the NMDA channel and calcium ions can then enter the cell to activate enzymes in the postsynaptic cell in a process that eventually leads to a de novo synthesis of AMPA receptors. Therefore, an ineffective synapse (that previously did not have AMPA receptors) begins synthesizing AMPA receptors after a strong noxious input. Consequently, this neuron will also respond to a normal nociceptive (nonpathologic) input.

Ongoing release of SP and glutamate will result in the activation of NMDA channels and influx of calcium in both excitatory and inhibitory neurons. However, the inhibitory neurons are smaller and undergo apoptosis, leading to an uninhibited segment. Furthermore, A Beta (β) fibers can also make novel synaptic connects with NK1 receptors, further driving this process.

Spinal facilitation is an increase in activity of spinal cord neurons due to the bombardment of nociceptive stimuli into dorsal horn neurons. Once nociceptors are sensitized they, in turn, can sensitize the dorsal horn neuron. Permanent damage might ensue. An under-appreciated anatomical fact is that afferent fibers actually trifurcate upon entering the dorsal horn and some visceral afferents

have been found to span the entire length of the spinal cord. Based on this, consider the following clinical scenario:

An individual develops acute, severe painful cholecystitis. The sustained noxious input was sufficient to wipe out the inhibitory neurons at that segmental level (T6). However, the gall bladder is removed, completely alleviating the pain. Years later, the individual develops a minor back injury while shoveling snow. Now, afferent input enters L5-S1, and ascends the cord. Upon reaching the T6 segment (that has lost its inhibitory neuron), it activates this segmental level and causes the identical pain pattern caused by the cholecystitis years before. For this reason, osteopathy considers the reemergence of an old pain pattern as the possible harbinger of new disease.

UNCOVERING THE BIOCHEMICAL MILIEU OF MYOFASCIAL TRIGGER POINTS

Myofascial pain associated with MTrPs is a common cause of nonarticular musculoskeletal pain. It is responsible for much suffering and expense. The presence of MTrPs can be determined by soft tissue palpation, but its pathogenesis has remained elusive. This author's team at NIH designed a clinical protocol to assess the local biochemical milieu of MTrPs. This team fabricated and tested a novel, 32-gauge microdialysis needle capable of collecting small volumes (~ 0.5 µl), and sub-nanogram levels of solutes less than 75k Da from muscle tissue. This enabled the study of the local trigger point milieu in subjects with and without MTrPs, and with and without pain in the upper trapezius muscle.

In this study, three subjects were selected based on history and physical examination to be in each of three groups (a total of nine subjects). Group 1was defined as "normal" (no neck pain, no MTrP); Group 2 was defined as "latent" (no neck pain, MTrP present); and Group 3 was defined as "active" (neck pain, MTrP present). Samples were obtained continuously with the microdialysis needle at regular intervals, including needle insertion, elicitation of a local twitch response, and posttwitch.

Main outcome measures were levels of pH, SP, CGRP, BK, 5-HT, norepinephrine, tumor necrosis factor alpha (TNF-α) Interleukin-1β (IL-1β) determined by analysis of samples.

Oerall the amounts of SP, CGRP, BK, 5-HT, norepinephrine, TNF-α and IL-1β were found to be significantly higher in the active group than either of the other two groups ($p<.01$). Overall, pH was significantly lower in the active group than the other two groups ($p<.03$). In the *Active* group, the amounts of SP and CGRP were significantly lower at the end of sampling (posttwitch) than at baseline ($p<.02$).

This novel microanalytical technique enables continuous, real-time sampling of extremely small quantities of small substances directly from soft tissue, with minimal system perturbation. It was found that subjects with neck pain secondary to a myofascial trigger point in the upper trapezius had significantly elevated levels of the aforementioned substances in the local muscle biochemical milieu compared to carefully matched controls. These findings were published in the *Journal of Applied Physiology*.[7] The local biochemical milieu does appear to change with a local twitch response. These findings are elucidating the pathogenesis, persistence and amplification of myofasical pain.

CONCLUSION

Ongoing advances in molecular and cellular biological methods and knowledge of the unique properties of the neuraxis are fundamentally changing our understanding of chronic pain mechanisms. Active MTrPs function as dynamic foci of peripheral nociception that can initiate, accentuate, and maintain central sensitization and chronic pain states. Continuous nociceptive input from MTrPs can increase excitability of dorsal horn neurons (causing allodynia and hyperalgesia) and open ineffective synapses - resulting in new receptive fields and referral of pain.

Trigger point acupuncture is an effective technique for deactivating MTrPs. Uncovering the biochemical profile of active MTrPs and determining the local effects of needle insertion may help elucidate mechanisms behind the initiation and amplification of myofascial pain, allowing targeted pharmacologic treatments at those mechanisms. It may also explain how acupuncture and other physical modalities work at the local level.

REFERENCES

1. Carlson CR, Okeson JP, Falace DA, Nitz AJ, Lindroth JE. Reduction of pain and EMG activity in the masseter region by trapezius trigger point injection. Pain 1993;55:397-400.
2. Hoheisel U, Koch K, Mense S. Functional reorganization in the rat dorsal horn during an experimental myositis. Pain 1994;59:111-118.
3. Hopwood MB, Abram SE. Factors associated with failure of trigger point injections. Clin J Pain 1994;10:227-234.
4. Melzack R, Stillwell DM, Fox EJ. Trigger points and acupuncture points for pain: correlations and implications. Pain 1977;3:3-23.
5. Mense S, Simons DG. Muscle Pain: Understanding Its Nature, Diagnosis and Treatment. Baltimore: Lippincott, Williams and Wilkins, 2001.
6. Nelson LS, Hoffman RS. Intrathecal injection: unusual complication of trigger-point injection therapy. Ann Emerg Med 1998;32:506-508.

7. Shah, JP, Phillips TM, Danoff JV, Gerber LH. An in vivo microanalytical technique for measuring the local biochemical milieu of human skeletal muscle. J Appl Physiol 2005;99:1977-1984.
8. Simons DG, Travell, JG, Simons LS. Travell and Simons' myofascial pain and dysfunction: the trigger point manual, volume 1. Upper half of body. Baltimore: Williams and Wilkins; 1999.
9. Wall PD, Woolf CJ. Muscle but not cutaneous C-afferent input produces prolonged increases in the excitability of the flexion reflex in the rat. J Physiol. 356:443-58, 1984.

Paraneoplastic Neurological Autoimmunity

Vanda A. Lennon, MD, PhD

Director
Neuroimmunology Laboratory and Autoimmune Neurology Fellowship Program
Departments of Neurology, Immunology, and Laboratory Medicine and Pathology
Mayo Clinic
Rochester, Minnesota

INTRODUCTION

It has long been recognized that certain subacute neurological disorders reflect a remote effect of systemic cancer. Paraneoplastic neurological disorders are considered rare and, in North America, are currently diagnosed more commonly in women than in men. In the past two decades these disorders are acknowledged to be a manifestation of neurological autoimmunity.[24] Endogenous antigens derived from a remote neoplasm, either new or recurrent, initiate these immune responses. The patient's neurological symptoms are not due to metastases which are, in fact, uncommon beyond regional lymph nodes because the immune response causing the neurological symptoms is very effective at limiting tumor spread. Neurological symptoms generally precede cancer detection. The most frequently detected neoplasms are small-cell lung carcinoma, carcinomas of breast and gynecologic (mullerian), seminoma, thymoma, Hodgkin's lymphoma and, in children, neuroblastoma. In 15% of patients, a coexisting but unrelated neoplasm is found before detection of the neoplasm predicted by the patient's serum autoantibody profile. The most common of the first encountered (but irrelevant) cancers in patients with paraneoplastic autoimmunity related to small-cell lung carcinoma are carcinomas of prostate, breast, colon, rectum, kidney and skin (basal cell and squamous cell), melanoma, chronic lymphocytic leukemia, and non-Hodgkin's lymphoma.

In a patient presenting with unexplained subacute neurological symptoms, the profile of onconeural autoantibodies in serum or spinal fluid aids the diagnosis of paraneoplastic neurological disorders and can predict, with high probability, the underlying neoplasm that initiated the immune response targeting the nervous system. The autoantibody predictors of cancer defined in the past two decades reflect a multi-faceted immune response mounted against a nonobvious systemic cancer. Predominantly of immunoglobulin G (IgG) class, they are specific for nuclear antigens expressed in neurons or glia, cytoplasmic antigens expressed in neurons, glia or muscle, or plasma membrane antigens expressed in neurons or muscle. Tables 1 and 2 list oncological and neurological associations of these antibodies. Antigens that are restricted to the intracellular compartment are not displayed constitutively on the surface of tumor cells, neurons or muscle cells, but under the influence of pro-inflammatory cytokines such as IFNγ, major histocompatibilty complex (MHC) class 1 molecules bearing peptides derived from the intracellular compartment are exported to the cell surface. Thus, MHC class 1 molecules containing autoantigenic peptides are made accessible to activated peptide-specific CD8+ cytotoxic T-cells that permeate all tissues in the course of immune surveillance. In contrast, integral plasma membrane proteins, such as cation channels in neuromuscular and autonomic synapses, are readily accessible to circulating autoantibodies.

Neurologists since the early 20th century have considered paraneoplastic disorders to have syndromic presentations. Sensory neuronopathy and subacute cerebellar ataxia are well-known examples. Marketing literature in the 1990s perpetuated the erroneous assumption that distinctive paraneoplastic autoantibodies signified specific neurological syndromes. However, Mayo Clinic experience has affirmed that syndromic presentations account for only a mi-

nority of paraneoplastic disorders.[21] These disorders are typically multifocal and at onset are mistaken for vascular, inflammatory, or degenerative disorders. Prompt and comprehensive serological evaluation facilitates early diagnosis and favors a better outcome by permitting early initiation of immunomodulatory therapy and the identification and treatment of the underlying, and usually unsuspected, neoplasm.[15]

COMMONLY ENCOUNTERED NEOPLASMS

Table 1 lists autoantibody profiles that predict specific cancer types. Table 2 reveals that the neurological accompaniments of these marker autoantibodies often involve multiple levels of the nervous system.[4,5,9,17,35,40] To date, small-cell lung carcinoma (SCLC) is the most commonly identified cancer in both men and women with paraneoplastic neurological autoimmunity. In men, the second most commonly recognized neoplasms are thymoma, seminoma, and Hodgkin's lymphoma.[3,7,31] In women, breast carcinoma follows SCLC in frequency, then thymoma, ovarian and other mullerian ductal carcinomas, and ovarian teratomas.[13,22,23,38] Lymphoproliferative neoplasms are encountered in men and women. In children, neuroblastomas are the most commonly recognized cancers associated with neurological autoimmunity. Paraneoplastic disorders that predominantly affect peripheral nerve have been reported in patients with multiple myeloma and Waldenström macroglobulinemia.

Table 1 Autoantibody markers of cancer

Cancer	Marker autoantibodies recognized to date
Lung carcinoma:	
small-cell type	ANNA-1, ANNA-2, ANNA 3, AGNA, CRMP-5, amphiphysin, PCA-2, striational, Zic4,[2] VGCC (N-type and P/Q-type), VGKC, ganglionic AChR, muscle AChR
non-small-cell type	VGCC (N-type), striational, muscle AChR, ganglionic AChR
Thymoma	Muscle AChR, striational, GAD65, CRMP-5, VGKC,[31] ganglionic AChR ANNA-1
Breast, ductal	ANNA-2, amphiphysin, VGCC (N-type), muscle AChR
Ovarian	PCA-1, VGCC (N-type > P/Q type), muscle AChR, EFA6A*
Mullerian ductal	
Testicular neoplasms	Ma2
Hodgkin's lymphoma	PCA-Tr; mGluR1[25]
Neuroblastoma	ANNA-1, muscle AChR, VGCC (N-type), striational

*Marker of ovarian teratoma[38]

AGNA = anti-glial nuclear antibody; ANNA = anti-neuronal nuclear autoantibody; CRMP= collapsin response-mediator protein; VGCC = neuronal voltage-gated calcium channel; VGKC = neuronal voltage-gated potassium channel; PCA = Purkinje cell cytoplasmic autoantibody; GAD65 = glutamic acid decarboxylase (65 kDa isoform); AChR = acetylcholine receptor

NEUROLOGICAL CLUES

Before referral to a neurologist, patients with a paraneoplastic autoimmune neurological disorder often present to rheumatologists, gastroenterologists, psychiatrists, physiatrists, or ophthalmologists. Most have neurological symptoms of subacute onset and lack symptoms or signs of cancer, which typically is diagnosed months later. In some patients, several years elapse before the pertinent cancer is diagnosed. Important diagnostic clues include a past history or family history of cancer or autoimmunity, and a history of smoking, occupational or social exposure to tobacco smoke, or exposure to other carcinogens, particularly asbestos.

Neurologists traditionally regard paraneoplastic disorders as syndromic with each syndrome having a specific autoantibody marker. For example, the antineuronal nuclear autoantibody-type 1 (ANNA-1, or "anti-Hu") was reported initially in patients with sensory neuronopathy related to SCLC, the Purkinje cell cytoplasmic autoantibody-type 1 (PCA-1, or "anti-Yo") was first recognized in women with cerebellar ataxia related to ovarian carcinoma, ANNA-2 (or "anti-Ri") was first reported in women with opsoclonus/myoclonus related to breast carcinoma, and amphiphysin autoantibody was first reported in women with "stiff-man syndrome" related to breast carcinoma. Continuing experience reveals that paraneoplastic autoantibodies often coexist and define a single tumor, and that the neurological presentation is multifocal and variable.[21] Table 2 lists the neurological symptoms and signs of paraneoplastic autoimmunity from the electrodiagnostic physician's perspective.

Peripheral Nervous System

Muscle

Visceral neoplasia is diagnosed in 9% to 15% of patients presenting with polymyositis or dermatomyositis. Skin symptoms usually precede muscle weakness. Interstitial lung disease, serum creatinine kinase (CK) elevation, detection of Jo-1 antibody, and electromyography (EMG) findings aid the diagnosis.[6] Acute necrotizing myopathy, presenting with painful proximal muscle weakness, has been reported with carcinoma of the lung, breast, kidney, stomach,

Table 2 Neurological manifestations by anatomical level involved and associated autoantibodies

Level	Disorder	Autoantibody markers
Muscle	Polymyositis/dermatomyositis	Anti-Jo[6]
Neuromuscular junction	Lambert-Eaton Myasthenic Syndrome	VGCC (P/Q-type > N-type) > AGNA10 > muscle AChR or striational = ganglionic AChR > VGKC. Neuronal nuclear and cytoplasmic antibodies are rare without other neurological accompaniments.
	Myasthenia gravis	Muscle AChR > striational > CRMP-5 > VGKC > ganglionic AChR
Peripheral somatic nerves and ganglia	Sensory neuronopathy & sensorimotor neuropathies	ANNA-1 > CRMP-5 > VGCC > ganglionic AChR, amphiphysin, muscle AChR, striational
Autonomic and enteric nervous system	Dysautonomias	Ganglionic AChR, muscle AChR, VGCC (N-type), VGKC, striational > ANNA-1 > CRMP-5 > VGCC (P/Q-type)
	Gastrointestinal dysmotilities	VGCC (N-type >> P/Q-type), ganglionic AChR, muscle AChR > ANNA 1 > CRMP-5
Spinal cord	Myelopathy, myoclonus	VGCC = CRMP-5 > amphiphysin > ganglionic AChR > VGKC > ANNA-2 = ANNA-1
Cranial nerves	Special senses, bulbar, motor neuropathies	CRMP-5 > ANNA-1 = VGCC (N-type > P/Q-type) > muscle and ganglionic AChR and striational
Brainstem	Brainstem encephalitis	VGCC (P/Q-type or N-type), CRMP-5, PCA 2, ANNA-1, muscle AChR, ganglionic AChR, ANNA-2, amphiphysin, Ma2.
	Stiff-person phenomena	Amphiphysin IgG (39% of women and 12% of men).
Cerebellum	Cerebellar ataxia	PCA-1 and PCA-Tr: symptoms predominantly involve cerebellum or connections; CRMP-5, VGCC (P/Q-type or N-type), PCA-2, ganglionic AChR, muscle AChR, ANNA-1: symptoms usually multifocal
Basal Ganglia	Chorea	Multiple autoantibodies; syndromic association with CRMP-5
	Myoclonus	Multiple autoantibodies
Diencephalon	Hypothalamic dysfunction	Ma2 > ANNA-1
Cerebral Cortex	Limbic encephalitis	CRMP-5, ANNA-1, VGCC, VGKC,[27,37] Ma2, amphiphysin, EFA6A[38] muscle AChR, ganglionic AChR
	Neuropsychiatric disorder	VGKC, VGCC, muscle AChR, ganglionic AChR, striational, CRMP-5 > amphiphysin > ANNA-2 > ANNA-1 > PCA-1

AChR = acetylcholine receptor; AGID = autoimmune gastrointestinal dysmotility; AGNA = anti-glial nuclear antibody; ANNA = anti-neuronal nuclear autoantibody; ARF6 = ADP-ribosylation factor 6; CAR = cancer (SCLC)-associated retinopathy; CD4+ = peptide-specific helper T lymphocyte (Th) and effector of delayed hypersensitivity responses; CD8+ = peptide-specific cytotoxic effector T lymphocyte; CK = creatinine kinase; CRMP-5 = neuronal collapsin response mediator protein; CT = computed tomography; EFA6A = exchange factor for ARF6; GI = gastrointestinal;GAD65= glutamic acid decarboxylase (65 kDa isoform); LEMS, Lambert-Eaton myasthenic síndrome; MHC = major histocompatibility complex; NMO = neuromyelitis optica; SCLC = small-cell lung carcinoma; PCA = Purkinje cell cytoplasmic autoantibody; PET = positron emission tomography; IVIg = intravenous immune globulin therapy; VGCC = neuronal voltage-gated calcium channel; VGKC, neuronal voltage-gated potassium channel

colon, pancreas, or prostate. Serum CK is elevated and biopsy demonstrates muscle necrosis with minor inflammation. Pharyngeal or respiratory muscle weakness is usually fatal.

Neuromuscular Junction

The Lambert-Eaton myasthenic syndrome (LEMS) is a presynaptic disorder of peripheral cholinergic neuromuscular transmission accompanied by limited dysautonomia.[12] It presents insidiously as proximal limb weakness with strength improving after several seconds of sustained voluntary contraction. Electromyographic characteristics and seropositivity for neuronal Ca^{2+} channel autoantibodies distinguish LEMS from myasthenia gravis (MG). It is underappreciated that 13% of LEMS patients are seropositive for muscle acetylcholine receptor (AChR) or striational antibodies.[16] However, patients with MG are seronegative for Ca^{2+} channel antibodies except in rare non-thymomatous paraneoplastic cases. The P/Q-type Ca^{2+} channel antibody is detected in 90% of non-immunosuppressed LEMS patients and is the presumptive effector of LEMS.[14] Approximately 60% of LEMS patients have SCLC and LEMS is estimated to affect 1%-2% of patients with SCLC. Dysautonomia in LEMS characteristically impairs tearing, salivation, sweating, and penile erection. When accompanied by other autonomic manifestations (e.g., gastrointestinal dysmotility or orthostatism) or sensory phenomena (e.g., pain in the low back, buttocks, and thighs), the autoantibody profile usually indicates coexistence of paraneoplastic autonomic neuropathy or radiculoneuropathy. For example, AGNA, ANNA-1, amphiphysin, or CRMP-5-IgG may be positive in addition to P/Q-type Ca^{2+} channel antibody, with or without N-type Ca^{2+} channel antibody.[10,16,17]

The postsynaptic neuromuscular transmission defect of MG is caused by antibodies directed at the extracellular domain of muscle AChR. Common symptoms are fatigable weakness of extremities and oculobulbar muscles. Thymoma is detected in about 15% of adult patients. Other neoplasms are documented infrequently. Distinctive autoantibody profiles that predict thymoma differ from profiles predictive of SCLC (Table 1) by lacking Ca^{2+} channel antibodies.[31] Neuromyotonia, rippling muscle disease, and cramp-fasciculation syndrome represent a continuum of acquired presynaptic disorders of continuous muscle fiber activity and are frequently associated with thymoma or SCLC.[29]

Roots, Ganglia, and Nerves

Peripheral neuropathy is the most common manifestation of paraneoplastic neurological autoimmunity. Subacute sensory neuronopathy is a classical presentation of autoimmunity related to SCLC, but the most common presentation is a sensorimotor neuropathy. Sensory neuropathy, considered a syndromic manifestation of ANNA-1 autoimmunity, affects 40% of ANNA-1 positive patients. Collapsin response mediator protein (CRMP)-5-IgG, N-type calcium $(Ca)^{2+}$ channel and ganglionic AChR antibodies also are common autoantibody markers of sensory neuronopathy (Table 2). Motor and autonomic neurons or their synapses may be involved in isolation or in association with a sensory neuronopathy. Approximately 10% of patients with Waldenström macroglobulinemia have sensory neuropathy.

Mononeuropathies, plexopathies, polyradiculopathies and small-fiber neuropathies may occur in isolation or in a multifocal presentation. An acute, rapidly progressive, sensorimotor polyneuropathy resembling Guillain-Barré syndrome (or its Miller-Fisher variant) is encountered with SCLC and less commonly with Hodgkin's lymphoma. Multiple myeloma is accompanied by a slowly progressive sensorimotor neuropathy in about 10% of patients. With osteosclerotic myeloma, approximately 50% of patients are estimated to develop a predominantly motor neuropathy similar to chronic inflammatory demyelinating polyneuropathy. Vasculitis restricted to nerve or muscle is reported with lymphoma, leukemia, and carcinoma of the prostate, kidney, lung, and endometrium. It presents as a symmetric or asymmetric, painful, sensorimotor neuropathy with proximal muscle weakness. Positive findings on biopsy of muscle (microvasculitis) or nerve (intramural and perivascular inflammatory infiltrates) confirms the diagnosis

Autonomic Nervous System

Autoimmune autonomic neuropathy or ganglionopathy is usually a component of a multifocal neurological disorder associated with SCLC or thymoma. Less common oncological associations include neoplasms of pancreas, testis and ovary, carcinoid, and lymphoma. Orthostatic hypotension and anhidrosis are prominent signs of sympathetic failure. Dry mouth, erectile dysfunction, impaired pupillary response to light and accommodation, and a fixed heart rate are evidence of parasympathetic failure.[33] The isolated symptoms and signs of autoimmune gastrointestinal (GI) dysmotility (AGID) are underappreciated manifestations of paraneoplastic dysautonomia and are usually attributed to "cancer cachexia."[19,40] Clues to gastroparesis include anorexia, early satiety, postprandial abdominal pain and vomiting. Constipation may progress to pseudo-obstruction, and diarrhea may be prominent. Isolated achalasia, dysphagia, pyloric stenosis, and anal spasticity have been encountered.[19] The enteric nervous system is typically infiltrated by T-cells.[18] Signs of somatic motor and sensory nerve dysfunction may be minimal or absent. Table 2 summarizes the autoantibodies that are currently recognized as markers of paraneoplastic AGID.

Paraneoplastic AGID often coexists with a multifocal neurological presentation. Its diagnosis depends largely on an informative autoantibody profile and confirmation by formal studies of GI motility. To date, the only proven effector of autoimmune dysautonomia is the ganglionic AChR antibody.[30] Other autoantibody markers that are diagnostically useful include: muscle AChR and striational

antibodies, neuronal nuclear and neuronal cytoplasmic antibodies (particularly ANNA-1 and CRMP-5 IgG), neuronal voltage-gated Ca^{2+} channel antibodies (N-type > P/Q type), and neuronal voltage-gated potassium (K)+ channel antibody.

Spinal Cord

Numerous neuronal nuclear and cytoplasmic autoantibodies serve as markers of paraneoplastic myelopathy (Table 2). The typical presentation is subacute with prominent motor involvement. Symptoms and signs of autoimmune motor neuron disease resemble those of amyotrophic lateral sclerosis. Involvement of multiple levels of the neuroaxis is a helpful guide to the diagnosis of paraneoplastic motor neuropathy. Dual involvement of optic nerves and spinal cord is syndromic for CRMP-5 autoimmunity which tends to be misdiagnosed as multiple sclerosis or neuromyelitis optica (NMO or Devic's disease).[5] Neuromyelitis optica-IgG, an autoantibody specific for the predominant water channel protein of the central nervous system, aquaporin-4, is a valuable marker of an underappreciated nonparaneoplastic autoimmune myelopathy. Seropositivity for NMO-IgG predicts with greater than 50% certainty a relapse of myelopathy or development of optic neuritis within 12 months.[39]

Cranial Nerves and Ganglia

Optic Nerve and Retina

Paraneoplastic autoimmune vision loss related to SCLC is identified most commonly by the CRMP-5-IgG autoantibody.[5] The characteristic ophthalmologic presentation is a combination of optic neuritis and retinitis with vitreous and intrathecal inflammation. Other reported paraneoplastic disorders of vision are encountered less frequently. These include cancer (SCLC)-associated retinopathy, and melanoma-associated retinopathy.[11]

Other Cranial Nerves

Cranial neuropathies in paraneoplastic cases are more frequently multiple than isolated. The most frequent marker autoantibody is CRMP-5-IgG (Table 2). Common symptoms include abnormalities of smell, taste or eye movement, facial weakness, numbness and pain, deafness, tinnitus, vestibular dysfunction, and dysphagia.[40] Subacute hearing loss is the most common cranial neuropathy encountered in ANNA-1 seropositive patients with SCLC19 and in association with thymoma.[31]

Brainstem

Ophthalmoplegia and movement disorders (parkinsonian tremor, rigidity, dystonia, and opsoclonus or myoclonus) are manifestations of midbrain and pontine encephalitis. Medullary involvement can cause nausea, vomiting, vertigo, nystagmus, ataxia, and bulbar palsy. Brainstem phenomena occur with ANNA-2 autoimmunity (71%),[22] Ma2 autoimmunity (73%)[20] and in lower frequency with other paraneoplastic autoantibodies (Table 2). Paraneoplastic "stiff-person" syndrome is characterized by severe, painful, and progressive muscle rigidity or stiffness that prominently affects the spine and lower extremities. Breast carcinoma and SCLC are the most frequently encountered neoplasms. Amphiphysin antibody is the most distinctive marker of paraneoplastic stiff-person syndrome; low titers of GAD65 antibody (<20 nmol/L) coexist with amphiphysin in 27% of patients.[23] The GAD65 antibody is the most frequent neuronal autoantibody recognized with thymoma.[31] A high serum level of GAD65 autoantibody (> 20 nmol/L) aids the diagnosis of classical stiff-person (Moersch-Woltmann) syndrome, which is usually idiopathic, but may accompany thymoma.

Extrapyramidal System

Paraneoplastic chorea, with basal ganglionic imaging abnormalities, is a syndromic manifestation of CRMP-5 autoimmunity related to SCLC.[35] It is commonly associated with subacute loss of vision, smell and taste, peripheral neuropathy, and limbic encephalitis.[40] Myoclonus is a more common paraneoplastic movement disorder. Less common are athetosis, parkinsonism, hemi-ballismus, tremor, dystonia, and blepharospasm.

Cerebellum

Subacute cerebellar ataxia frequently dominates a multifocal paraneoplastic neurological presentation. It is important to distinguish sensory ataxia from cerebellar ataxia. Cerebellar ataxia is the most common presentation of patients who are seropositive for PCA-1 (of whom 99% are women, with 90% having ovarian or breast carcinoma)[13] or PCA-Tr (a marker of Hodgkin's lymphoma).[3,32] Purkinje cell cytoplasmic autoantibody-1-positive patients have prominent cerebellar symptoms and signs in 90% of cases. However, 10% of PCA-1-positive patients present with neuropathic symptoms and signs as the sole neurological manifestation (motor more than sensory, and rarely autonomic).[28] Purkinje cell cytoplasmic autoantibody-1 is rarely, if ever, accompanied by neuronal nuclear or other neuronal cytoplasmic autoantibodies.[21] On the other hand, cerebellar ataxia related to SCLC or breast carcinoma is frequently accompanied by multiple autoantibodies yielding an informative serum profile predictive of the cancer (Tables 1 and 2).

Cerebral cortex

Paraneoplastic limbic encephalitis, characterized by memory impairment, seizures, and psychiatric manifestations, is most commonly associated with SCLC (70% of cases). The serum autoantibody profile is variable (Table 2). Some patients present with subacute dementia. Others present neuropsychiatrically with mental status change and behavioral abnormalities. Women with cerebral cortical presentations may have ovarian teratoma, the diagnosis of which is aided by detection of an adenoside5-diphosphate-ribosylation factor (ARF6) exchange factor (EFA6A) specific autoantibody.[38]

Diencephalon

Paraneoplastic narcolepsy differs from idiopathic narcolepsy by having accompaniments of limbic or brainstem encephalitis or endocrinopathies. Low (or undetectable) cerebral spinal fluid hypocretin levels reflect hypothalamic involvement. Ma2[20] and ANNA-1 autoantibody (unpublished data) are markers of this disorder.

ANCILLARY TESTS

Autoantibody Profiles

Optimal evaluation for paraneoplastic autoimmunity requires broad screening for serum antibodies reactive with onconeural antigens shared by cancer cells, neurons, glia or muscle. Diagnostically important autoantibodies are often missed when testing is limited to a single or nominal number of individual antibodies.[21] ANNA-2 and amphiphysin-IgG, for example, were recognized initially in women with breast carcinoma, but when accompanied by ANNA-1, ANNA-3, CRMP-5-IgG, PCA-2 or anti-glial nuclear antibody (AGNA), the serological profile has high specificity for SCLC.

Although a negative autoantibody profile does not exclude paraneoplastic autoimmunity, an informative autoantibody profile: (1) confirms an autoimmune etiology; (2) focuses the search for cancer in the context of the patient's risk factors; (3) explains neurological symptoms appearing in the course or wake of cancer therapy that are not attributable to metastasis; (4) differentiates autoimmune neuropathies from neurotoxic effects of chemotherapy; (5) allows monitoring of the immune response in the course of cancer therapy; and (6) may herald cancer recurrence in previously seropositive patients. Initially seronegative patients may later convert to seropositive. Autoantibody profiles in an individual patient evolve with time. Thus, in the absence of cancer therapy or immunotherapy, serological re-evaluation is advisable at 4-6 month intervals when no cancer is found at initial workup and the suspicion for a paraneoplastic disorder remains high.

Other Laboratory Investigations

Customary signs of malignancy (anemia, elevated erythrocyte sedimentation rate, tumor mass, ascites, pleural effusion, or abnormal liver function tests [reflecting metastasis]) are characteristically lacking in patients presenting with paraneoplastic neurological autoimmunity. Patients with SCLC are often hyponatremic, which may be a manifestation of the neoplasm's secretion of ectopic antidiuretic hormone or may be due to autoimmune hypothalamitis. Hypothyroidism, type-1 diabetes, and nonneurological autoantibodies (both organ-specific and nonorgan-specific) are all valuable clues to an autoimmune process.

The clinical findings may justify EMG, nerve conduction studies, electroencephalography, and MRI imaging of the brain and spinal cord. An inflammatory spinal fluid with leukocytosis (usually < 50 cells/mL with predominant lymphocytosis) and elevated protein (with or without supernumerary oligoclonal IgG bands) support an inflammatory disorder of the CNS. Autoantibodies are sometimes detectable in the spinal fluid and not in the serum (i.e., CRMP-5-IgG).

Cancer Search

Conventional imaging may be negative because neoplasms associated with autoimmunity are usually limited. Subtle abnormalities should be investigated further. For chest evaluation, computed tomography (CT) is recommended in the first instance.[36] Positron emission tomography (PET) is an alternative diagnostic tool to evaluate mediastinal lymph nodes. Computed tomography of the abdomen and pelvis are helpful in identifying primary visceral malignancies and metastases. If radiological investigation fails to indicate abnormality, whole-body PET (rather than thorax-restricted PET) may locate an extrapulmonary small-cell carcinoma. Tissue diagnosis should be pursued aggressively when a thoracic lesion or lymphadenopathy is identified. More than one cancer is encountered in approximately 15% of patients with paraneoplastic autoimmunity related to SCLC.[19,40]

When the autoantibody profile suggests breast carcinoma, regular self-examination is most important. Subtle mammographic abnormalities should be biopsied in surveillance of patients without definitive breast imaging abnormality. Breast MRI or sonography are sometimes helpful. Evaluation of gynecological cancer status may require sonography of the pelvis in addition to CT and manual pelvic examination. For PCA-1-positive patients whose breast evaluation, pelvic imaging and examination, and serum CA125 levels are all normal, exploratory laparotomy often reveals pelvic carcinoma (ovarian, fallopian tubal, or serous surface papillary adenocarcinoma).[13] Testicular ultrasonography is a most important test for men with subacute brainstem encephalitis, whether or not Ma2 antibody is detected.

PATHOGENESIS OF PARANEOPLASTIC NEUROLOGICAL DISORDERS

Onconeural proteins expressed in the plasma membrane, nucleus or cytoplasm of certain neoplasms initiate tumor-targeted responses.[15,17] Corresponding antigenic proteins expressed in neurons, glia, or muscle are coincidental targets. Autoantibodies themselves can cause disease when directed at the extracellular domain of plasma membrane antigens in muscle or neurons, as exemplified by MG, LEMS, and autoimmune dysautomonia.[14,30] However, nuclear and cytoplasmic antigens are not accessible to immune attack in healthy cells. Autoantibodies of nuclear and cytoplasmic specificities serve as surrogate markers for activation of CD8+ cytotoxic T-cells that are activated by peptides derived from the interior of tumor cells. These T-cells limit the tumor's spread. However, when peptides derived from corresponding proteins inside neurons

and glia are displayed on MHC class-I molecules that are upregulated in a pro-inflammatory cytokine milieu, they are accessible to peptide-specific effector T-cells.

The principles accounting for autoimmune neurological disorders are illustrated by two disorders with contrasting immune mechanisms. The presynaptic neurotransmission defect that is characteristic of LEMS related to SCLC is caused by neuronal P/Q-type Ca^{2+} channel IgG. This disorder is not inflammatory, and accordingly, the pathogenicity of P/Q-type calcium channel antibodies at motor nerve terminals does not require complement activation.[14] In contrast is the inflammatory response mediated by cytotoxic T-cells that cause cerebellar degeneration related to ovarian carcinoma. Although not cytotoxic to cerebellar neurons in vivo, the PCA-1 autoantibody is predominantly of the complement-activating IgG1 subclass, and the presence of this subclass correlates significantly with neurological morbidity.[26] This association implies that the cytokine milieu prevailing at the tumor site of initial $CD4^+$ helper T-cell activation favored a pro-inflammatory (TH1) response. Albert and colleagues demonstrated circulating $CD8^+$ cytotoxic T-cells specific for a synthetic peptide of PCA-1 sequence in a patient with recent onset paraneoplastic cerebellar degeneration.1 Furthermore, patients with chronic paraneoplastic cerebellar degeneration had circulating peptide-specific $CD4^+$ memory T-cells that, upon in vitro activation by PCA-1 peptide, yielded antigen-specific $CD8^+$ cytotoxic T-cells.

THERAPEUTIC CONSIDERATIONS

Mayo Clinic observations suggest that ablation of an efficacious tumor immune response by myelosuppressive therapy (e.g., cisplatin and etoposide) may adversely affect tumor outcome in seropositive patients.[8] Nonneurological patients with limited SCLC had an impressive 41% frequency of neuronal autoantibodies at cancer diagnosis. In contrast, only 17% in patients with extensive cancer at outset had these autoantibodies. However, survival did not differ in the two groups after standard chemotherapy. In unpublished observations, striking cases of rapid cancer dissemination following initiation of severely immunosuppressing chemotherapies after years of stable imaging evidence of cancer have been encountered. Less immunosuppressant agents, such as cyclophosphamide, appear to be more beneficial in patients with paraneoplastic autoimmunity.[34] Therapeutic trials are urgently needed to determine optimal anti-tumor therapy for patients whose serological profile is indicative of a protective immune response.

There is also need for optimization of immunotherapeutic protocols to treat neurological dysfunction in these patients. When the response to acute treatment with high-dose IV methylprednisolone, IVIg, or plasmapheresis is beneficial, consideration of maintenance immunosuppression with oral azathioprine, or cyclophosphamide is justified. Promising therapies include mycophenylate mofetil, rituximab (a humanized monoclonal antibody that depletes B cells) and agents targeting activated T-cells such as tacrolimus or natalizumab (a humanized monoclonal antibody against leukocyte $\alpha 4$ integrins). Immunomodulatory therapy generally is not effective for inflammatory parenchymal syndromes. Nevertheless, variable and sometimes dramatic improvements have been reported anecdotally. In general, syndromes thought to be mediated by IgG (e.g. limbic encephalitis associated with neuronal voltage-gated K^+ channel antibody, LEMS associated with P/Q-type Ca^{2+} channel antibody, and cerebellar ataxia associated with various cation channel antibodies) are more likely to respond to steroid, IVIg, or plasmapheresis than disorders associated with ANNA-1, CRMP-5 or PCA-1 autoantibodies which are thought to be mediated by cytotoxic effector T-cells.[1]

Long-term outcome is optimized by careful attention to rehabilitation (physiotherapy, occupational therapy and speech therapy), supportive care (respiratory and nutritional) and medical management of neurological symptoms (e.g., pyridostigmine or 3,4-diaminopyridine for LEMS; high doses of benzodiazepines for stiff-person syndrome or stiff-person phenomena and antiepileptic medications, such as sodium valproate or clonazepam, for opsoclonus myoclonus). Neuropsychiatric manifestations may respond remarkably to corticosteroid therapy or neuroleptic medications. Pain, both central and peripheral, is a frequent and largely intractable complaint, but may respond to low-dose tricyclic antidepressants, gabapentin or opiates.

SUMMARY

Certain subacute neurological disorders reflect a remote effect of systemic cancer. Paraneoplastic neurological disorders are diagnosed more commonly in women than in men. Endogenous antigens derived from a remote neoplasm, either new or recurrent, initiate these immune responses. Neurological symptoms generally precede cancer detection. The most frequently detected neoplasms are small-cell lung carcinoma, carcinomas of breast and gynecologic (mullerian), seminoma, thymoma, Hodgkin's lymphoma and, in children, neuroblastoma. Prompt and comprehensive serological evaluation facilitates early diagnosis and favors a better outcome.

REFERENCES

1. Albert ML, Darnell JC, Bender A, Francisco LM, Bhardwaj N, Darnell RB. Tumor-specific killer cells in paraneoplastic cerebellar degeneration. Nat Med 1998;4:1321-1324.
2. Bataller L, Wade DF, Graus F, Stacey HD, Rosenfeld MR, Dalmau J. Antibodies to Zic4 in paraneoplastic neurological disorders and small-cell lung cancer. Neurology 2004;62:778-782.

3. Bernal F, Shams'ili S, Rojas I, Sanchez-Valle R, Saiz A, Dalmau J, et al. Anti-Tr antibodies as markers of paraneoplastic cerebellar degeneration and Hodgkin's disease. Neurology 2003;60:230-234.
4. Chan KH, Vernino S, Lennon VA. ANNA-3 anti-neuronal nuclear antibody: marker of lung cancer-related autoimmunity. Ann Neurol 2001;50:301-311.
5. Cross SA, Salomao DR, Parisi JE, Kryzer TJ, Bradley EA, Mines JA, Lam BL, Lennon VA. Paraneoplastic autoimmune optic neuritis with retinitis defined by CRMP-5-IgG. Ann Neurol 2003;54:38-50.
6. Dalakas MC. Immunopathogenesis of inflammatory myopathies. Ann Neurol 1995;37:S74-S75.
7. Dalmau J, Graus F, Villarejo A, Posner JB, Blumenthal D, Thiessen B, Saiz A, Meneses P, Rosenfeld MR. Clinical analysis of anti-Ma-2-associated encephalitis. Brain 2004;127:1831-1844.
8. Galanis E, Frytak S, Rowland KM, Sloan JA, Lennon VA. Neuronal autoantibody titers in the course of small cell lung carcinoma and platinum associated neuropathy. Cancer Immunol Immunother 1999;48:85-90.
9. Graus F, Dalmau J, Rene R, Tora M, Malats N, Verschuuren JJ, et al. Anti-Hu antibodies in patients with small-cell lung cancer: association with complete response to therapy and improved survival. J Clin Oncol 1997;15:2866-2872.
10. Graus F, Vincent A, Pozo-Rosich P, Sabater L, Saiz A, Lang B, Dalmau J. Anti-glial nuclear antibody: marker of lung cancer-related paraneoplastic neurological syndromes. J Neuroimmunol 2005;165:166-171.
11. Guy J, Aptsiauri N. Treatment of paraneoplastic visual loss with intravenous immunoglobulin: a report of 3 cases. Arch Ophthalmol 1999;117:471-477.
12. Harper CM, Lennon VA. Lambert-Eaton syndrome. In: Kaminski HJ, editor. Current clinical neurology: myasthenia gravis and related disorders. Totowa, NJ: Humana Press; 2002. p 269-291.
13. Hetzel D, Stanhope CR, O'Neill BP, Lennon VA. Gynecologic cancer in patients with subacute cerebellar degeneration predicted by anti-Purkinje cell antibodies and limited in metastatic volume. Mayo Clin Proc 1990;65:1558-1623.
14. Lambert EH, Lennon VA. Selected IgG rapidly induces Lambert-Eaton myasthenic syndrome in mice: Complement independence and EMG abnormalities. Muscle Nerve 1998;11:1133-1145.
15. Lennon VA. Calcium channel and related paraneoplastic disease autoantibodies. In: Peter JB, Schoenfeld Y, editors. Textbook of autoantibodies. Amsterdam: Elsevier Science, 1996:139-147.
16. Lennon VA. Serological profile of myasthenia gravis and distinction from the Lambert-Eaton myasthenic syndrome. Neurology 1997;48: S23-S27.
17. Lennon VA, Kryzer TJ, Griesmann GE, O'Suilleabhain PE, Windebank AJ, Woppmann A, Miljanich GP, Lambert EH. Calcium-channel antibodies in the Lambert-Eaton syndrome and other paraneoplastic syndromes. N Engl J Med 1995;332:1467-1474.
18. Lennon VA, Sas DF, Busk MF, Scheithauer B, Malagelada JR, Camilleri M, Miller LJ. Enteric neuronal autoantibodies in pseudo-obstruction with small cell lung carcinoma. Gastroenterology 1991;200:137-142.
19. Lucchinetti CF, Kimmel DW, Lennon VA. Paraneoplastic and oncological profiles of patients seropositive for type 1 anti-neuronal nuclear antibodies. Neurology 1998;50:652-657.
20. Overeem S, Dalmau J, Bataller L, Nishino S, Mignot E, Verschuuren J, Lammers GJ. Hypocretin-1 CSF levels in anti-Ma2 associated encephalitis. Neurology 2004;62:138-140.
21. Pittock SJ, Kryzer TJ, Lennon VA. Paraneoplastic antibodies coexist and predict cancer, not neurological syndrome. Ann Neurol 2004;56:715-719.
22. Pittock SJ, Lucchinetti CF, Lennon VA. Anti-neuronal nuclear autoantibody type 2: paraneoplastic accompaniments. Ann Neurol 2003;53:580-597.
23. Pittock SJ, Lucchinetti CF, Parisi JE, Benarroch EE, Mokri B, Stephan CL, Kim KK, Kilimann MW, Lennon VA. Amphiphysin autoimmunity: paraneoplastic accompaniments. Ann Neurol 2005;58:96-107.
24. Rudnicki SA, Dalmau J. Paraneoplastic syndromes in the spinal cord, nerve, and muscle. Muscle Nerve 2000;23:1800-1818.
25. Sillevis Smitt P, Kinoshita A, De Leeuw B, Moll W, Coesmans M, Jaarsma D, et al. Paraneoplastic cerebellar ataxia due to autoantibodies against a glutamate receptor. N Engl J Med 2000;342:21-17.
26. Tavee J, Yu Z, O'Neill BP. PCA-1 autoantibody of IgG1 subclass predominates in patients with most severe paraneoplastic cerebellar degeneration. Neurology 2001;56:A415-416.
27. Thieben MJ, Lennon VA, Boeve BF, Aksamit AJ, Keegan M, Vernino S. Potentially reversible autoimmune limbic encephalitis with neuronal potassium channel antibody. Neurology 2004;62:1177-1182.
28. Tracy J, Lennon VA, Pittock SJ. Purkinje cell antibody type 1 (PCA-1; anti-Yo): peripheral nerve manifestations. Neurology 2006;66:A188.
29. Vernino S, Auger RG, Emslie-Smith AM, Harper CM, Lennon VA. Myasthenia, thymoma, presynaptic antibodies and a continuum of neuromuscular hyperexcitability. Neurology 1999;54:1233-1239.
30. Vernino S, Ermilov LG, Sha L, Szurszewski JH, Low PA, Lennon VA. Passive transfer of autoimmune autonomic neuropathy to mice. J Neurosci 2004;24:7037-7042.
31. Vernino S, Lennon VA. Autoantibody profiles and neurological correlations of thymoma. Clin Cancer Res 2004;10:7270-7275.
32. Vernino S, Lennon VA. New Purkinje cell antibody (PCA-2): marker of lung cancer-related neurological autoimmunity. Ann Neurol 2000;47:397-305.
33. Vernino S, Low PA, Fealey RD, Stewart JD, Farrugia G, Lennon VA. Autoantibodies to ganglionic acetylcholine receptors in autoimmune autonomic neuropathies. N Engl J Med 2000;343:847-855.
34. Vernino S, O'Neill BP, Marks RS, O'Fallon JR, Kimmel DW. Immunomodulatory treatment trial for paraneoplastic neurological disorders. Neuro-oncol 2003;6:55-62.

35. Vernino S, Tuite P, Adler CH, Meschia Jf, Boeve BF, Boasberg P, Parisi JE, Lennon VA. Paraneoplastic chorea associated with CRMP-5 neuronal antibody and lung carcinoma. Ann Neurol 2002;51:625-630.
36. Verschakelen JA, De Wever W, Bogaert J. Role of computed tomography in lung cancer staging. Curr Opin Pulm Med 2004;10:248-255.
37. Vincent A, Buckley C, Schott JM, Baker I, Dewar BK, Detert N, Clover L, Parkinson A, Bien CG, Omer S, Lang B, Rossor MN, Palace J. Potassium channel antibody-associated encephalopathy: a potentially immunotherapy-responsive form of limbic encephalitis. Brain 2004;127:701-712.
38. Vitaliani R, Mason W, Ances B, Zwerdling T, Jiang Z, Dalmau J. Paraneoplastic encephalitis, psychiatric symptoms, and hypoventilation in ovarian teratomas. Ann Neurol 2005;58:594-604.
39. Weinshenker BG, Wingerchuk DM, Vukusic S, Pittock SJ, Lucchinetti CF, Lennon VA. NMO-IgG predicts relapse following longitudinally extensive transverse myelitis. Ann Neurol 2006;59:566-569.
40. Yu Z, Kryzer TJ, Griesmann GE, Kim K, Benarroch EE, Lennon VA. CRMP-5 neuronal autoantibody: marker of lung cancer and thymoma-related autoimmunity. Ann Neurol 2001;49:146-154.

That which does not stabilize, will only make us stronger.

H. Kazerooni
Department of Mechanical Engineering
University of California, Berkeley
Berkeley, CA 94720, USA
exo@berkeley.edu

Abstract − In October 2003, the first functional load-bearing and energetically autonomous exoskeleton, called the Berkeley Lower Extremity Exoskeleton (BLEEX) was demonstrated, walking at the average speed of two miles per hour while carrying 75 pounds of load. BLEEX is a load-carrying and energetically autonomous human exoskeleton that, in this first generation prototype, carries up to a 34 kg (75 lb) payload for the pilot and allows the pilot to walk at up to 1.3 m/s (2.9 mph). This article focuses on the human-in-the-loop control scheme and the novel ring-based networked control architecture (ExoNET) that together enable BLEEX to support payload while safely moving in concert with the human pilot. The BLEEX sensitivity amplification control algorithm proposed here increases the closed loop system sensitivity to its wearer's forces and torques without any measurement from the wearer (such as force, position, or electromyogram signal). The tradeoffs between not having sensors to measure human variables, the need for dynamic model accuracy, and robustness to parameter uncertainty are described. ExoNET provides the physical network on which the BLEEX control algorithm runs. The ExoNET control network guarantees strict determinism, optimized data transfer for small data sizes, and flexibility in configuration. Its features and application on BLEEX are described.

I. INTRODUCTION

The goal of the exoskeleton project at U.C. Berkeley is to develop fundamental technologies associated with the design and control of energetically autonomous lower extremity exoskeletons that augment human strength and endurance during locomotion. The first generation lower extremity exoskeleton (commonly referred to as BLEEX) is comprised of two powered anthropomorphic legs, a power unit, and a backpack-like frame on which a variety of heavy loads can be mounted. This system provides its pilot (i.e. the wearer) the ability to carry significant loads on his/her back with minimal effort over any type of terrain. BLEEX allows the pilot to comfortably squat, bend, swing from side to side, twist, and walk on ascending and descending slopes, while also offering the ability to step over and under obstructions while carrying equipment and supplies. Because the pilot can carry significant loads for extended periods of time without reducing his/her agility, physical effectiveness increases significantly with the aid of this class of lower extremity exoskeletons.

BLEEX has numerous potential applications; it can provide soldiers, disaster relief workers, wildfire fighters, and other emergency personnel the ability to carry heavy loads such as food, rescue equipment, first-aid supplies, communications gear, and weaponry, without the strain typically associated with demanding labor. Unlike unrealistic fantasy-type concepts fueled by movie-makers and science-fiction writers, the lower extremity exoskeleton conceived at Berkeley is a practical, intelligent, load-carrying robotic device. BLEEX was first unveiled in 2004, at U.C. Berkeley's Human Engineering and Robotics Laboratory (Fig. 1). In this initial model, BLEEX offered a carrying capacity of 34 kg (75 lbs), with weight in excess of that allowance being supported by the pilot.

The effectiveness of the lower extremity exoskeleton is a direct result of the control system's ability to leverage the human intellect to provide balance, navigation, and path-planning while ensuring that the exoskeleton actuators provide most of the strength necessary for supporting payload and walking. In operation, the exoskeleton becomes transparent to the pilot and there is no need to train or learn any type of interface to use the robot. The control algorithm ensures that the exoskeleton always moves in concert with the pilot with minimal interaction force between the two and was first presented in [1]. The control scheme needs no direct measurements from the pilot or the human-machine interface (e.g. no force sensors between the two); instead, the controller estimates, based on measurements from the exoskeleton structure only, how to move so that the pilot feels very little force. This control scheme is an effective method of generating locomotion when the contact location between the pilot and the exoskeleton is unknown and unpredictable (i.e. the exoskeleton and the pilot are in contact in variety of places). This

control method differs from compliance control methods employed for upper extremity exoskeletons [2, 3 and 4], and haptic systems because it requires no force sensor between the wearer and the exoskeleton.

The basic principle for the control of BLEEX rests on the notion that the exoskeleton needs to shadow the wearer's voluntary and involuntary movements quickly, and without delay. This requires a high level of sensitivity in response to all forces and torques on the exoskeleton, particularly the forces imposed by the pilot. Addressing this need involves a direct conflict with control science's goal of minimizing system sensitivity in the design of a closed loop feedback system. If fitted with a low sensitivity, the exoskeleton would not move in concert with its wearer. We realize, however, that maximizing system sensitivity to external forces and torques leads to a loss of robustness in the system.

Fig. 1. Berkeley Lower Extremity Exoskeleton (BLEEX) first generation prototype and pilot.

Taking into account this new approach, our goal was to develop a control system for BLEEX with high sensitivity. We were faced with two realistic concerns; the first was that an exoskeleton with high sensitivity to external forces and torques would respond to other external forces not initiated by its pilot. The key to stabilizing the exoskeleton and preventing it from falling in response to external forces depends on the pilot's ability to move quickly (e.g. step back or sideways) to create a stable situation for himself and the exoskeleton. For this, a very wide control bandwidth is needed so the exoskeleton can respond to both pilot's voluntary and involuntary movements (i.e. reflexes). The second concern is that systems with high sensitivity to external forces and torques are not robust to variations and therefore the precision of the system performance will be proportional to the precision of the exoskeleton dynamic model. Although this is a serious drawback, we have accepted it as unavoidable. Nevertheless,

various experimental systems in our laboratory have proved the overall effectiveness of the control method in shadowing the pilot's movement.

Realization of this control scheme requires a high-performance physical control architecture. This paper presents the ring-based protocol and distributed networked control hardware called the ExoNet. Traditional centralized control architectures where a supervisory controller directly interfaces in a point-to-point fashion with all sensors and actuators in the system have been successfully implemented in the past. They are generally feasible when a controller interfaces with small number of sensors and actuators and requires short wiring to them. Larger sophisticated multi-degree-of-freedom systems frequently require the control network to be compact, easily reconfigurable, expandable, and maintainable. Hence, we utilized a networked control system (NCS) as an alternative to the conventional centralized control system because of its advantages in flexibility, volume of wiring and capacity of distribution.

II. Previous Work

In our research work at U.C. Berkeley, we have divided the technology associated with human power augmentation into lower extremity exoskeletons and upper extremity exoskeletons. The reason for this was two-fold; firstly, we could envision a great many applications for either a stand-alone lower or upper extremity exoskeleton in the immediate future. Secondly, and more importantly for the separation, is that the exoskeletons are in their early stages, and further research still needs to be conducted to ensure that the upper extremity exoskeleton and lower extremity exoskeleton can function well independently before we can venture an attempt to integrate them. See [6,7] for research work on upper extremity exoskeletons at Berkeley.

The concept of a powered human-assistive exoskeleton has been explored in various reach projects since the 1950's, though recent advances in controls and computation have generated renewed interest (see [8-11]). A recent notable project is the "RoboKnee," which is a powered knee brace that functions in parallel to the wearer's knee but does not transfer loads to the ground [12]. This device transfers the weight of the backpack payload onto the human skeleton (including shanks, ankles, and feet). "HAL", a walking aid system for individuals with gait disorders, is another current exoskeleton-like device in that it adds to the force generated by the human muscles but relies on the human skeleton to transfer loads [13]. BLEEX draws on this history of exoskeleton development but is unique in that it mechanically functions as a true load bearing exoskeleton, is energetically autonomous, and utilizes a unique control system that does not require any direct measurements on the human. Networked control systems (NCSs), such as the one developed for BLEEX, have broad applications beyond just exoskeleton control and have been adopted in fields related to industrial automation, building automation, office and home automation, intelligent vehicles, aircrafts, and spacecrafts [14-18]. Several network types had been developed based upon the applications, such as a process field bus (PROFIBUS) [19], manufacturing automation protocol (MAP) [20], and fiber distributed data interface (FDDI) [21].

III. Sensitivity Amplification Controller

A. A simple One Degree-of-Freedom (DOF) Example

The control of the exoskeleton is explained here through the 1 DOF example shown in Fig. 2. This figure schematically depicts a human leg attached and interacting with a 1 DOF exoskeleton leg in a swing configuration (no interaction with the ground). For simplicity, the exoskeleton leg is shown as a rigid link pivoting about a joint and powered by a single actuator. The exoskeleton leg in this example has an actuator that produces a torque, r, about pivot point A. Although the pilot is attached securely to the exoskeleton at the foot, other parts of the pilot leg, such as the shanks and thighs, can contact the exoskeleton and impose forces and torques on the exoskeleton leg. The location of the contacts and the direction of the contact forces (and sometimes contact torques) vary and are therefore considered unknown values in this analysis. In fact, one of the primary objectives in designing BLEEX was to ensure a pilot's unrestricted interaction with BLEEX. The equivalent torque on the exoskeleton leg, resulting from the pilot's applied forces and torques, is represented by d. Fig. 3 presents the system dynamics in block diagram form.

In the case where multiple actuators produce controlled torques on the system, r is the vector of torques imposed on the exoskeleton by the actuators. G is the transfer function from the actuator input, r, to the exoskeleton angular velocity, v (actuator dynamics are included in G). The form of G and the type of internal feedback for the actuator is immaterial for the discussion here. The Laplace operator has been omitted in all equations for the sake of compactness.

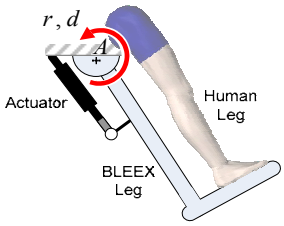

Fig. 2 One DOF conceptual model of an exoskeleton leg interacting with the pilot's leg.

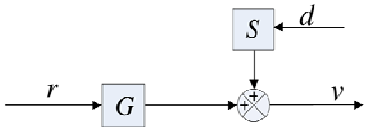

Fig. 3 The exoskeleton's angular velocity shown as a function of the input to the actuators, *r*, and the torques imposed by the pilot onto the exoskeleton, *d*.

The sensitivity transfer function S, represents how the equivalent human torque affects the exoskeleton angular velocity. S maps the equivalent pilot torque, *d*, onto the exoskeleton velocity, *v*. If the actuator already has some sort of primary stabilizing controller, the magnitude of S will be small and the exoskeleton will only have a small response to the imposed forces and torques from the pilot or any other source. For example, a high gain velocity controller in the actuator results in small S, and consequently a small exoskeleton response to forces and torques. Also, non-backdrivable actuators (e.g. large transmission ratios or servo-valves with overlapping spools) result in a small S which leads to a correspondingly small response to pilot forces and torques.

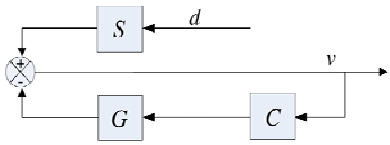

Fig. 4 Negative feedback control loop added to block diagram of Fig. 2 where *C* is the controller and it operates only on exoskeleton variables.

The resulting torque from pilot on the exoskeleton, *d*, is not an exogenous input; it is a function of the pilot dynamics and variables such as position and velocity of the pilot and the exoskeleton legs. These dynamics change from person to person, and within a person as a function of time and posture. These dynamics will be added to the analysis in later paragraphs, but they are unrelated to the purpose of current discussion. Our goal is to develop an exoskeleton with a large sensitivity to forces and torques from the operator using measurements only from the exoskeleton (i.e. no sensors on the pilot or the exoskeleton interface with the pilot). Creating a negative feedback loop from the exoskeleton variables only, as shown in Fig. 4, the closed-loop sensitivity transfer function is presented in (1).

$$S_{NEW} = \frac{v}{d} = \frac{S}{1 + GC} \qquad (1)$$

Observation of (1) reveals that $S_{NEW} \leq S$, and therefore any negative feedback from the exoskeleton leads to an even smaller sensitivity transfer function. With respect to (1), our goal is to design a controller for a given S and G such that the closed loop response from d to v (the new sensitivity function as given by (1)) is greater than the open loop sensitivity transfer function (i.e. S) within some bounded frequency range. This design specification is given by inequality (2).

$$|S_{NEW}| > |S| \qquad \forall \omega \in (0, \omega_O) \qquad (2)$$

or alternatively $|1 + GC| < 1 \qquad \forall \omega \in (0, \omega_O) \qquad (3)$

where ω_O is the exoskeleton maneuvering bandwidth.

Exoskeleton control requires a totally opposite goal from classical and modern control theory: *maximize the sensitivity of the closed loop system to forces and torques*. In classical servo problems, negative feedback loops with

large gains result in small sensitivity within a bandwidth, which means that they reject forces and torques (usually called disturbances). However, the above analysis states that the exoskeleton controller needs a large sensitivity to forces and torques. The exoskeleton controller uses the inverse of the exoskeleton dynamics as a positive feedback such that the loop gain for the exoskeleton approaches unity from below (slightly less than 1), which can be written as:

$$S_{NEW} = \frac{v}{d} = \frac{S}{1 - GC} \tag{4}$$

where *C* is chosen as $C = \left(1 - \alpha^{-1}\right)G^{-1}$ (5)

and α is the amplification number greater than unity.

If $\alpha = 10$, then $C = 0.9G^{-1}$, and the new sensitivity transfer function is $S_{NEW} = 10S$ (ten times the force amplification). Equation (5) simply states that a positive feedback controller needs to be chosen as the inverse dynamics of the system dynamics scaled down by $(1 - \alpha^{-1})$. Note that (5) prescribes the controller in the absence of unmodeled high-frequency exoskeleton dynamics. In practice, C also includes a unity gain low pass filter to attenuate the unmodeled high-frequency exoskeleton dynamics that may not be captured in the model, G^{-1}.

The success of this control method is dependant on the accuracy of system model (i.e. G^{-1}) which governs how much torque is needed at each joint to compensate for the payload and dynamics of the exoskeleton. Models errors which cause the exoskeleton to apply too little actuation torque mean that the pilot would feel a portion of the payload. Errors which cause over-actuation however, could lead to instability. This straightforward control solution comes with an expensive price: robustness to parameter variations. To get the above method working, one needs to know the dynamics of the system very well. The next section discusses this tradeoff.

B. Robustness to Parameter Variations

The variation in the new positive feedback sensitivity transfer function (4) is given by (6).

$$\frac{\Delta S_{NEW}}{S_{NEW}} = \frac{\Delta S}{S} + \frac{GC}{1 - GC}\frac{\Delta G}{G} \tag{6}$$

If GC is close to unity (when the force amplification number, α, is large) any parameter variation on modeling will be amplified as well. For example if the parameter uncertainty in the system is about 10%, i.e.: $\left|\frac{\Delta G}{G}\right| = 0.10$ and $\left|\frac{\Delta S}{S}\right| = 0$, then (6) results in

$$\left|\frac{\Delta S_{NEW}}{S_{NEW}}\right| = \left|\frac{GC}{1 - GC}\right| 0.10 \tag{7}$$

Now assume C is chosen such that $C = 0.9G^{-1}$. Substituting into (7) results in

$$\left|\frac{\Delta S_{NEW}}{S_{NEW}}\right| = 0.90 \tag{8}$$

Equation (8) indicates that any parameter variation directly affects the system behavior. In the above example, a 10% error in model parameters results in nine times the variation in the sensitivity function. This is why model accuracy is crucial to exoskeleton control. One can see this problem as a tradeoff: the design approach described above requires no sensor (e.g. force or electromyogram) in the interface between the pilot and the exoskeleton; one can push and pull against the exoskeleton in any direction and at any location without measuring any variables on the interface. However, the control method requires a very good model of the system. At this time, our experiments with BLEEX have shown that this control scheme—which does not stabilize BLEEX—forces the exoskeleton to follow wide-bandwidth human maneuvers while carrying heavy loads.

C. Pilot Dynamics

In our control scheme, as will be shown, there is no need to include the internal components of the pilot limb model; the detailed dynamics of nerve conduction, muscle contraction, and central nervous system processing are implicitly accounted for in constructing the dynamic model of the pilot limbs. For more detail on in-depth

modeling and analysis of the internal components of the pilot limb as applied to haptic systems and human power amplifiers, see [22,23] and our preliminary results in [24]. The pilot force on the exoskeleton, d, is a function of both the pilot dynamics, H, and the kinematics of the pilot limb (e.g., velocity, position or a combination thereof).

$$d = -H(v) \tag{9}$$

The specific form of H is not known other than that it results in the human muscle force on the exoskeleton. In general, H is determined primarily by the physical properties of the human dynamics. Here we assume H is a nonlinear operator representing the pilot impedance as a function of the pilot kinematics. Figure 5 represents the closed loop system behavior when pilot dynamics is added to the block diagram of Fig. 4. Examining Fig. 5 reveals that (4), representing the new exoskeleton sensitivity transfer function from *d* to *v*, is not affected by the feedback loop containing H. Figure 5 shows an important characteristic for human exoskeleton control: *two distinct feedback loops in the system*. The upper feedback loop represents how forces and torques from the pilot affect the exoskeleton and is internal to the human. The lower loop shows how the controlled feedback loop affects the exoskeleton. While the lower feedback loop is positive (potentially destabilizing), the upper human feedback loop stabilizes the overall system of pilot and exoskeleton taken as a whole.

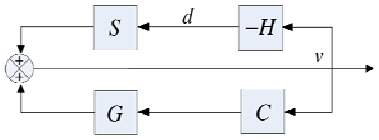

Fig. 5 The two feedback loops in this diagram represent the overall motion of the human and exoskeleton. The upper feedback loop shows how the pilot moves the exoskeleton through applied forces. The lower positive feedback loop shows how the controller drives the exoskeleton.

D. The Effect of Pilot Dynamics on Closed Loop Stability

How does the pilot dynamic behavior affect the exoskeleton behavior? In order to get an understanding of the system behavior in the presence of pilot dynamics we use our 1 DOF system and assume H is a linear transfer function. The stability of the system shown in Fig. 5 is decided by the closed-loop characteristic equation:

$$1 + SH - GC = 0 \tag{10}$$

In the absence of feedback controller, C, the pilot carries the entire load (payload plus the weight of the exoskeleton torso). The stability in this case is decided by the characteristic equation:

$$1 + SH = 0 \tag{11}$$

Characteristic equation (11) is always stable since it represents pilot coupled to a passive exoskeleton (i.e. no controller means $GC = 0$). When a feedback loop with C is added, the closed loop characteristic equation changes from (11) to (10), and using the Small Gain Theorem, one can show that the closed loop stability is guaranteed as long as inequality (12) is satisfied:

$$|GC| < |1 + SH| \qquad \forall \omega \in (0, \infty) \tag{12}$$

According to (5), C is chosen such that $|GC| < 1$ and therefore in the absence of uncertainties, (12) is guaranteed as long as $1 \leq |1 + SH|$. Unlike control methods utilized in the control of the upper extremity exoskeletons [4,25,26], the human dynamics in the control method described here has little potential to destabilize the system. Even though the feedback loop containing C is positive, the feedback loop containing H stabilizes the overall system of pilot and exoskeleton. The condition in (12) could be violated if $|GC| \geq 1$, which would result from model parameter uncertainties. In summary, the controller discussed here is stable when worn by the pilot as long as parameter uncertainties are kept to a minimum.

IV. Controller Implementation on BLEEX

A. Mechanical system

The above discussion motivated the design philosophy using a one DOF system. BLEEX, as shown in Fig. 1, is a system with many degrees of freedom and therefore implementation of BLEEX control deserves further attention. Each BLEEX leg has three DOFs at the hip, one DOF at the knee, and three DOFs at the ankle, of which only four are powered DOFs: hip, knee, and ankle joints in the sagittal plane and the hip abduction-adduction joints. See [24] for details of the BLEEX mechanical design. The pilot and BLEEX have rigid mechanical connections at the torso and the feet; everywhere else, the pilot and BLEEX have compliant or periodic contact. The connection at the torso is made using an adjustable compliant vest that distributes the forces between BLEEX and the pilot, thereby preventing abrasion. The vest includes a rigid plate (with hole pattern) on the back that bolts to the rigid metal spine of the BLEEX torso.

The pilot's shoes or boots attach to the BLEEX feet using a modified quick-release binding mechanism similar to snowboard bindings. The binding cleat on the modified pilot boot does not interfere with normal wear when the pilot is unclipped from BLEEX. The BLEEX foot is composed of a rigid heel section with the binding and a compliant, but load bearing, toe section that begins mid foot and extends to the toe. The BLEEX foot has a compressible rubber sole with a tread pattern that provides both shock-absorption and traction while walking. The rubber sole of the BLEEX foot contains multiple embedded pressure sensors (coarse on/off information only), that are used to detect the trajectory of the BLEEX ground reaction force starting from "heel-strike" to "toe-off" in the walking gait cycle. This information is used in the BLEEX controller to identify the BLEEX foot configuration relative to the ground.

BLEEX is powered via a compact portable hybrid output power supply contained in the backpack. Several different portable BLEEX power supplies have been designed by our group for different applications and environments. Each provides hydraulic flow and pressure for the actuators and generates electric power for the sensors, network, and control computer. Details of the design, testing, and performance of the BLEEX power supplies can be found in [27].

B. Dynamic Modeling

Although biomechanical studies of walking frequently identify seven or more distinct phases of the human walking gait cycle [28], for simplicity in control we consider BLEEX to have three distinct phases (shown in Fig. 6) which manifest to three different dynamic models:

Single support: one leg is in the stance configuration while another leg is in swing.

Double support: both legs are in stance configuration and situated flat on the ground.

Double support with one redundancy: both legs are in stance configuration, but one leg is situated flat on the ground while the other one is not.

Using the information from the sensors in the foot sole, the controller determines in which phase BLEEX is operating and which of the three dynamic models apply.

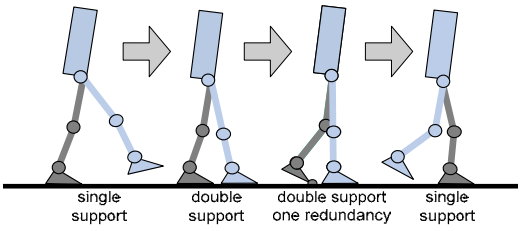

Fig. 6 Three phases of the BLEEX walking cycle.

In our initial control design process, we decoupled the control of the abduction-adduction DOF at the hip from the control of joints in the sagittal plane. This is valid because we noticed through measurements that the abduction-adduction movements during normal walking (less than 0.9 m/s or 2 mph) are rather slow [29]. In comparison with the movements in the sagittal plane, the abduction-adduction movements can be considered quasi-static maneuvers with little dynamical affects on the rest of system. For the sake of brevity, the following sections describe the control method in the sagittal plane for a given set of abduction-adduction angles.

C. Single Support

In the single support phase, BLEEX is modeled as the seven DOF serial link mechanism in the sagittal plane shown in Fig. 7. The dynamics of BLEEX can be written in the general form as:

$$M(\theta)\ddot{\theta} + C(\theta,\dot{\theta})\dot{\theta} + P(\theta) = T + d \qquad (13)$$

where

$\theta = \begin{bmatrix}\theta_1 & \theta_2 \ldots \theta_7\end{bmatrix}^T$ and $T = \begin{bmatrix}0 & T_1 & T_2 \ldots T_6\end{bmatrix}^T$.

M is a 7×7 inertia matrix and is a function of θ, $C(\theta,\dot{\theta})$ is a 7×7 centripetal and Coriolis matrix and is a function of θ and $\dot{\theta}$, and P is a 7×1 vector of gravitational torques and is a function of θ only. T is the 7×1 actuator torque vector with its first element set to zero since there is no actuator associated with joint angle θ_1 (i.e. angle between the BLEEX foot and the ground). d is the effective 7×1 torque vector imposed by the pilot on BLEEX at various locations. According to (5), we choose the controller to be the inverse of the BLEEX dynamics scaled by $(1-\alpha^{-1})$, where α is the amplification number.

$$T = \hat{P}(\theta) + (1-\alpha^{-1})\left[\hat{M}(\theta)\ddot{\theta} + \hat{C}(\theta,\dot{\theta})\dot{\theta}\right] \qquad (14)$$

$\hat{C}(\theta,\dot{\theta})$, $\hat{P}(\theta)$ and $\hat{M}(\theta)$ are the estimates of the Coriolis matrix, gravity vector, and the inertia matrix respectively for the system shown in Fig. 7. Note that (14) results in a 7×1 actuator torque. Since there is no actuator between the BLEEX foot and the ground, the torque prescribed by the first element of T must be provided by the pilot. Substituting T from (14) into (13) yields,

$$M(\theta)\ddot{\theta} + C(\theta,\dot{\theta})\dot{\theta} + P(\theta) = \hat{P}(\theta) + (1-\alpha^{-1})\left[\hat{M}(\theta)\ddot{\theta} + \hat{C}(\theta,\dot{\theta})\dot{\theta}\right] + d \qquad (15)$$

In the limit when $M(\theta) = \hat{M}(\theta)$, $C(\theta,\dot{\theta}) = \hat{C}(\theta,\dot{\theta})$, $P(\theta) = \hat{P}(\theta)$, and α is sufficiently large, d will approach zero, meaning the pilot can walk as if BLEEX did not exist. However, it can be seen from (15) that the force felt by the pilot is a function of α and the accuracy of the estimates $\hat{C}(\theta,\dot{\theta})$, $\hat{P}(\theta)$, and $\hat{M}(\theta)$. In general, the more accurately the system is modeled, the less the human force, d, will be. In the presence of variations in abduction-adduction angles, only $P(\theta)$ in equations (13) and (14) needs to be modified.

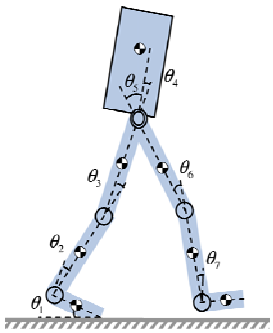

Fig.7 Sagittal plane representation of BLEEX in the single stance phase.

D. Double Support

In the double support phase, both BLEEX feet are flat on the ground. The exoskeleton is modeled as two planar 3 DOF serial link mechanisms that are connected to each other along their uppermost link as shown in Fig. 8-a. The dynamics for these serial links are represented by (16) and (17).

$$M_L(m_{TL},\theta_L)\ddot{\theta}_L + C_L\left(m_{TL},\dot{\theta}_L,\theta_L\right)\dot{\theta}_L + P_L(m_{TL},\theta_L) = T_L + d_L \qquad (16)$$

$$M_R(m_{TR},\theta_R)\ddot{\theta}_R + C_R\left(m_{TR},\dot{\theta}_R,\theta_R\right)\dot{\theta}_R + P_R(m_{TR},\theta_R) = T_R + d_R \qquad (17)$$

where: $\theta_L = \begin{bmatrix} \theta_{L1} & \theta_{L2} & \theta_{L3} \end{bmatrix}^T$ and $\theta_R = \begin{bmatrix} \theta_{R1} & \theta_{R2} & \theta_{R3} \end{bmatrix}^T$. m_{TR} and m_{TL} are effective torso masses supported by each leg and m_T is the total torso mass such that:

$$m_T = m_{TR} + m_{TL} \tag{18}$$

The contributions of m_T on each leg (i.e., m_{TL} and m_{TR}) are chosen as functions of the location of the torso center of mass relative to the locations of the ankles such that:

$$\frac{m_{TR}}{m_{TL}} = \frac{x_{TL}}{x_{TR}} \tag{19}$$

where x_{TL} is the horizontal distance between the torso center of mass and the left ankle, and x_{TR} is the horizontal distance between the torso center of mass and the right ankle. For example, if the center of mass of the torso is located directly above the right leg, then $m_{TL} = 0$ and $m_{TR} = m_T$. Similar to the single stance phase, the controllers are chosen such that

$$T_L = \hat{P}_L(m_{TL}, \theta_L) + (1 - \alpha^{-1})\left[\hat{M}_L(m_{TL}, \theta_L)\,\ddot{\theta}_L + \hat{C}_L(m_{TL}, \theta_L, \dot{\theta}_L)\dot{\theta}_L\right] \tag{20}$$

$$T_R = \hat{P}_R(m_{TR}, \theta_R) + (1 - \alpha^{-1})\left[\hat{M}_R(m_{TR}, \theta_R)\,\ddot{\theta}_R + \hat{C}_R(m_{TR}, \theta_R, \dot{\theta}_R)\dot{\theta}_R\right] \tag{21}$$

Needless to say, (19) is valid only for quasi-static conditions where the accelerations and velocities are small. This is in fact the case, since in the double support phase, both legs are on the ground and BLEEX's angular acceleration and velocities are quite small. This allows us to simplify (20) and (21) during slow walking by removing all terms except the estimates of the gravitational vectors.

E. Double Support with One Redundancy

Double support with one redundancy is modeled as a 3 DOF serial link mechanism for the stance leg with the foot flat on the ground and a 4 DOF serial link mechanism for the stance leg that is not completely on the ground (Fig. 8-b). Each serial link supports a portion of the torso weight. The dynamics for these serial links are similar to (16) and (17), with the exception that the redundant leg equation represents four DOFs as opposed to three. For the specific instant shown in Fig. 8-b, the left leg has 4 DOF and the right leg has 3 DOF.

Similar to the double support case, the effective torso mass supported by each leg is computed by (19). Controllers for this case can be chosen in the same manner as (20) and (21). Note that the actuator torque vector associated with the leg that has 4 DOF (e.g. T_L for the case shown in Fig. 8-b) is a 4×1 vector. As in the single support phase, the torque prescribed by the first element of T must be provided by the pilot because there is no actuator between the BLEEX foot and the ground. As the pilot walks, BLEEX transitions through the various phases shown in Fig. 6. The foot sole pressure sensors detect which leg has four degrees of freedom and which leg has three degrees of freedom and the controller then chooses the appropriate algorithm for each leg.

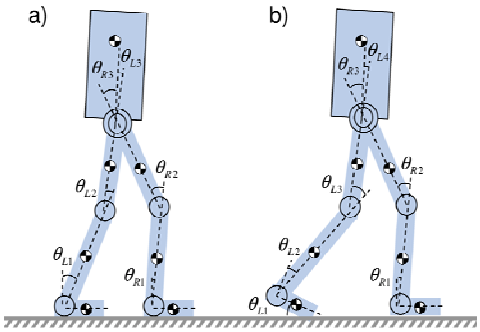

Fig. 8 Sagittal plane representation of BLEEX in a) the double support phase and b) the double support phase with one redundancy.

V. NETWORKED CONTROL SYSTEM

A. Network Structure

Fig. 9 provides global picture of the ExoNET networked control system that hosts the control algorithm. ExoNET was designed for BLEEX to enable the central controller to interact with distributed sensors, reduce the bulk, complexity, and difficulty of wiring, and achieve high-speed real-time control. ExoNET consists of four ring networks (ExoRing0~3). Each ring has a series of sensor and actuator data aggregation network nodes we call Remote I/O Modules, or RIOMs. Also, an additional network (GuiRing) provides a graphical user interface (GUI) for debugging and can be hot-swapped into the system while the network is running. These five networks are all served by a central module (ExoBrain) composed of a single board computer (ExoCPU), a PCI Interface Module (ExoPCI) and a Supervisor I/O Module (SIOM). The SIOM is a custom built board that has three independent transceiver channels. Channel 1 contains the two leg network rings: ExoRing0 and ExoRing2. Channel 2 contains the two torso network rings: ExoRing1 and ExoRing3. The third transceiver channel is coupled to GUI network (GuiRing).

The GUI network allows for real-time monitoring and administration of the control system for debugging purposes. The GUI network includes the GUI RIOM (GuiRIOM), the GUI PCI interface module (GuiPCI) and the GUI computer (GuiPC) inside the GUI computer case. The GuiRIOM and the GuiPCI stack together on a PCI riser card that is plugged into one of PCI slots of the GuiPC. Fig. 10 shows the ExoNET ring topology of an ExoRing where N RIOMs (Slave 1,2,…N) are serially connected to one SIOM (Master). Each serial link consists of three twisted pairs of wires. While the first and second pairs are used for receiving and transmitting data, the third pair is used for carrying power to RIOMs. The direction of data flow in this network is from the transmit port (TX) of the master node to the receive port (RX) of the Slave 1 node, and from the TX of the Slave 1 node to the RX of the Slave 2 node, and so forth. This path continues to the RX of the Slave N node. A loop-back terminator completes the ring by plugging into the TX of the Slave-N node so that data leaving from the TX of the Slave-N node will arrive at the RX of the SIOM master node after passing through each slave node internal loop line (labeled LP in Fig. 10).

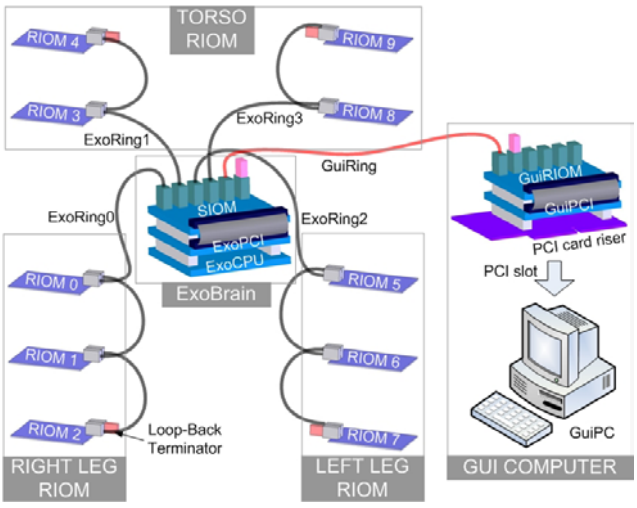

Fig. 9 Overall view of ExoNET networked control system and external GUI debug terminal.

This ring topology provides flexibility and expandability for the network: a user can easily add or remove slave nodes and then plug a loop-back terminator at the last slave node to complete the network. This topology eliminates the requirement of a single circulating serial cable connecting from the last slave node to the master node. It is particularly useful in cabling a network where all nodes are physically oriented on a line (as on the BLEEX legs). In this case, only one serial link cable between any two consecutive nodes and a loop-back terminator on the last node are required to form a complete ring network.

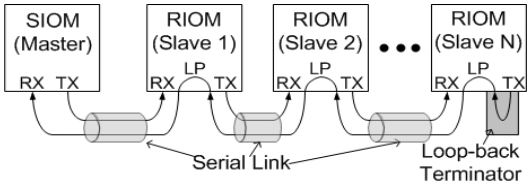

Fig. 10 Ring Topology

B. Remote I/O Modules (RIOMS) – A Practical Solution to Managing Wiring Complexity

The ExoNET RIOM modules (Fig. 11) act as smart sensor and control data aggregation nodes. BLEEX is a complex multi-degree of freedom device with a large number of sensor inputs and control outputs. A common approach in robotic design would be to route all sensor and actuator signal wires directly to a central control computer. For BLEEX, this would have meant a total of over 210 wires. By distributing network nodes around the robot, we only require one wire per limb (ring network) to route all sensor and actuation information. Each node takes care of interfacing with the various types of sensors (serial, parallel, analog, digital, etc…) located physically close by it and assembles the data into digital packets that can be transmitted via the network to-from the central computer. In addition, the RIOM can send out analog control signals for actuation (e.g. controlling a hydraulic servo-valve). The distribution and location of RIOMs is generally chosen to achieve a minimum volume of wiring and a reasonable and convenient allocation of sensors and actuators to each RIOM.

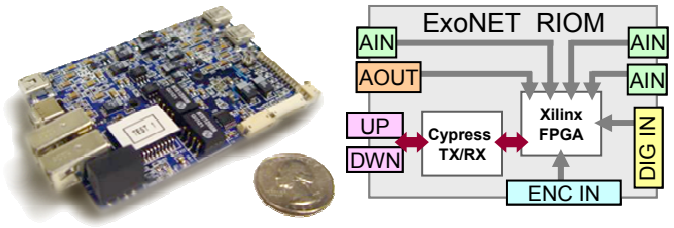

Fig. 11 ExoNET RIOM photo and schematic. Each RIOM provides for 3 analog inputs (AIN), 1 analog output (AOUT), 6 digital inputs (DIG IN), 1 quadrature encoder input (ENC IN), and 2 network communication ports (UP and DWN). Two integrated circuits handle processing (Xilinx Inc.) and network communication (Cypress Semiconductor Inc.) respectively.

Each RIOM in the first generation BLEEX provides five sensor inputs (three 16-bit analog inputs, one quadrature encoder input, and one 6-bit digital input) and one 16-bit analog actuation output. Details of the electronics hardware design can be found in [30]. Each link includes a pair of linear accelerometers that are connected to two of the analog input channels. When spaced out along a limb and read in differentially, these provide angular rate data for the controller. Each link is also responsible for recording data from an angular encoder at its proximal joint through the encoder channel. The remaining digital input channels are used on the foot links for capturing footswitch data that corresponds to the ground contact location. The analog output channel is used to send the control signal to the hydraulic servo-valve on an actuator.

C. Network Protocol

ExoNET network communication consists of passing "messages" around the ring formed by the nodes on the network (SIOM and RIOMs). A message is a series of data packets that is preceded by a chosen start delimiter code ("S" in Fig. 12) and proceeded by a chosen end delimiter code ("E" in Fig. 12). Each data packet in a message includes bits that indicate the source of the packet (e.g. the ID# of a RIOM), the type of data (e.g. error, sensor, actuation command,…), the actual data value, and error checking bits based on a cyclic redundancy check (CRC). Fig 12 shows two types of data packets in the message being passed between nodes: actuator commands sent from the master to the RIOMs (C1, C2), and sensor data destined for the master that was collected by the RIOMs (T11, T12, T21,…). Each communication cycle in the network protocol (Fig. 12) involves passing a message sequentially from the master node (e.g. a SIOM) to each slave node in the ring network (e.g. the RIOMs) and then returning the message back to the master node. As the message travels around the ring, each RIOM reads its assigned actuator command data packet (by looking for its RIOM ID#), and then appends its collected sensor data to the message. When the message returns to the master, completing the ring, it has grown to include the sensor data from each node in the network. Because the communication cycles occur at a fixed rate set by the control scheme, this protocol allows for deterministic control and provides built in network error detection because every message returning to the master must contain information from each node on the ring.

Testing ExoNET on BLEEX has shown that the network update time (NUT) for a ten RIOM network, passing 140 bytes of data, takes less than 20μs. The controller for BLEEX updates at 2 kHz (500 μs sample time), which leaves 480μs to perform the control algorithm calculations on the ExoCPU. For a more detailed discussion of the BLEEX control network and performance analysis, see [30,31].

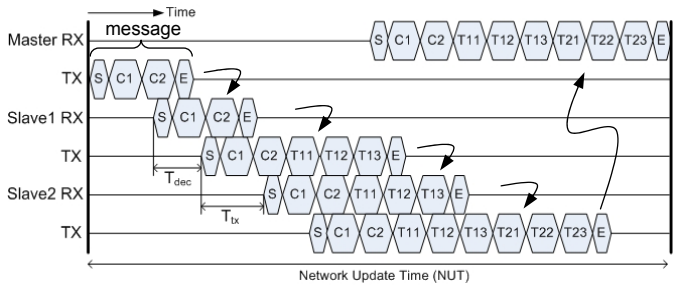

Fig. 12 Network communication overview. In a communication cycle, messages (strings of data packets beginning with start delimiter, S, and ending with end delimiter, E) pass from a master node (SIOM) to each slave node (RIOM) sequentially and return to the master node to complete the ring network communication

VI. HIGHLIGHTS OF THE BLEEX DESIGN

In designing BLEEX, several factors had to be considered: Firstly, the exoskeleton needed to exist in the same workspace of the pilot without interfering with his motion. Secondly, it had to be decided whether the exoskeleton should be anthropomorphic (i.e., kinematically matching), or non-anthropomorphic (i.e. kinematically matching the operator only at the connection points between human and machine). We ultimately selected the anthropomorphic architecture because of its transparency to the pilot. We also concluded that an exoskeleton that kinematically matches the wearer's legs gains the most psychological acceptance by the user and is therefore safer to wear. Consequently, the exoskeleton was designed to have the same degrees of freedom as the pilot: three degrees at the ankle and the hip, and one degree at the knee. This architecture also allowed the appropriately scaled clinical human walking data to be employed for design of the exoskeleton components, including the workspace, actuators and the power source.

A study of clinical gait analysis (CGA) data provides evidence that humans expend the most power through the sagittal plane joints of the ankle, knee, and hip while walking, squatting, climbing stairs, and most other common maneuvers. For this reason, the sagittal plane joints of the first prototype exoskeleton are powered. However, to save energy, the non-sagittal degrees of freedom at the ankle and hip remain unpowered. This compels the pilot to provide the force to maneuver the exoskeleton abduction and rotation, where the required operational forces are smaller. To further reduce the burden on the human operator, the unactuated degrees of freedom are spring-loaded to a neutral standing position. Using CGA data and human factors information, the ranges of motion for the exoskeleton were selected to be larger than those of the human while walking, and smaller than the physical limit of the human joints. This ensures sufficient flexibility for walking, while maintaining the safety of the pilot. In order to accommodate the largest number of pilots, the exoskeleton was designed to have adjustable shank and thigh sections. These sections will adjust from 5% to 95% of the shank and thigh length of men in the U.S. Army as determined from the human factors literature. At the foot, the exoskeleton rigidly attaches to the pilot's boot with a binding, but a flexible toe-section, ankle abduction, and vertical rotation axis allow the exoskeleton foot sufficient maneuverability to keep from encumbering the user.

The hips connect the legs to the torso through three degrees of freedom. Among these three degrees of freedom, only one degree in the sagital plane is powered. The exoskeleton torso is a structural member that rigidly connects to the pilot vest. The vest is designed from several hard Polycarbonate surfaces connected compliantly together to conform to the pilot's chest, shoulders and upper back, thereby preventing concentrated forces between the exoskeleton and the wearer. The torso also provides mounting points for the power supply, payload and computer. The Clinical Gait Analysis (CGA) was used to provide not only the basis for the exoskeleton kinematics and dynamic architecture, but also for its actuation. The deployment of this CGA data was motivated by the assumption that BLEEX resembles a human's weight and volume. The BLEEX ankle actuators were designed to provide relatively large plantarflexion torques (~1000 lb-in) corresponding to those needed for propulsion at toe-off. The knee actuators were designed to provide both large extension torques (~800 lb-in) needed during heel strike, which occurs while walking, and large flexion torques (~-800 lb-in) needed during swing, which occurs with actions like climbing stairs. The hip actuators were designed to provide relatively symmetric flexion and extension torques (+/- 900 lb-in) corresponding to the symmetric nature of the torques required at the hip to walk. These critical design decisions were further reinforced by physiological observation. Since hydraulic linear actuators were employed to power the BLEEX joints, the imposed torque at each joint was a nonlinear function of the actuator location and its geometry. An optimization code was written to locate both the actuator endpoint locations and the area of the cross section of the actuators so as to yield the right amount of torque at each joint. If the actuators were designed to yield a large amount of torque more than what is prescribed by CGA data at each joint, then there would be a great amount of power loss during modulation (e.g. control).

CGA data, which provided torque and speed information at each joint of a 165 pound person, was also used to size the exoskeleton power source. The information suggested that a typical person uses about 0.25 HP (185 Watts) to walk at average speed of 3 mph. This figure, which represents the average product of speed and torque, is an expression of the purely mechanical power exhibited at the legs during walking. Since we assumed that the exoskeleton is similar to a human in terms of geometry and weight, one of the key design objectives turned out to be designing a power unit and actuation system to deliver about 0.25 HP at the exoskeleton joints.

VII. CONCLUSION

The Berkeley Lower Extremity Exoskeleton (BLEEX) is not a typical servo-mechanism. While providing disturbance rejection along some axes preventing motion in response to gravitational forces, BLEEX actually encourages motion along other axes in response to pilot interface forces. This characteristic requires large sensitivity to pilot forces which invalidates certain assumptions of the standard control design methodologies, and thus requires a new design approach. The controller described here uses the inverse dynamics of the exoskeleton as a positive feedback controller so that the loop gain for the exoskeleton approaches unity (slightly less than 1). Our current experiments with BLEEX have shown that this control scheme has two superior characteristics: 1) it allows for wide bandwidth maneuvers; 2) it is unaffected by changing human dynamics. The trade off is that it requires a relatively accurate model of the system. The ExoNET control network that hosts the control algorithm is also presented. Video clips which demonstrate BLEEX, the control network, and the effectiveness of the control scheme can be found at http://bleex.me.berkeley.edu/bleex.

VIII. REFERENCES

[1] H. Kazerooni, J.L. Racine, H. Huang, and R. Steger, “On the Control of the Berkeley Lower Extremity Exoskeleton (BLEEX),” IEEE Int. Conf. Robotics and Automation, Barcelona, Spain, Apr. 2005.

[2] H. Kazerooni, and S. Mahoney, "Dynamics and Control of Robotic Systems Worn By Humans," ASME Journal of Dynamic Systems, Measurements, and Control, vol. 113, no. 3, Sept. 1991.

[3] H. Kazerooni, "Human-Robot Interaction via the Transfer of Power and Information Signals," IEEE Transactions on Systems and Cybernetics, vol. 20, no. 2, Apr. 1990, pp. 450-463.

[4] H. Kazerooni, and J. Guo, "Human Extenders," ASME Journal of Dynamic Systems, Measurements, and Control, vol. 115, no. 2B, June 1993, pp 281-289.

[5] H. Kazerooni, R. Steger, "The Berkeley Lower Extremity Exoskeletons", ASME Journal of Dynamics Systems, Measurements and Control, V128, March 2006

[6] H. Kazerooni, and M. Her, "The Dynamics and Control of a Haptic Interface Device," IEEE Transactions on Robotics and Automation, vol. 10, no. 4, Aug. 1994, pp 453-464.

[7] H. Kazerooni, and T. Snyder, "A Case Study on Dynamics of Haptic Devices: Human Induced Instability in Powered Hand Controllers," AIAA J. of Guidance, Control, and Dynamics, vol. 18, no. 1, 1995.

[8] B.J. Makinson, and General Electric Co., “Research and Development for Machine Augmentation of Human Strength and Endurance, Hardiman I Project,” General Electric Report S-71-1056, Schenectady, NY, 1971.

[9] M. Vukobratovic, D. Hristic, and Z. Stojiljkovic, “Development of Active Anthropomorphic Exoskeletons,” Medical and Biological Engineering, Jan. 1974, pp. 66-80.

[10] K. Yamamoto, K. Hyodo, M. Ishii, and T. Matsuo, “Development of Power Assisting Suit for Assistng Nurse Labor,” JSME International Journal Series C., vol. 45, No. 3, Sep. 2002.

[11] P. Neuhaus, and H. Kazerooni, “Industrial-Strength Human-Assisted Walking Robots”, IEEE Robotics and Automation Magazine, vol. 8, no. 4., Dec. 2001, pp. 18-25.

[12] J. Pratt, B. Krupp, C. Morse, and S. Collins, “The RoboKnee: An Exoskeleton for Enhancing Strength During Walking”, IEEE Conf. on Robotics and Aut., New Orleans, Apr. 2004.

[13] H. Kawamoto, and Y. Sankai, “Power Assist System HAL-3 for gait Disorder Person”, ICCHP, Austria, July 2002.

[14] S. Biegacki and D. VanGompel, “The application of DeviceNet in process control”, ISA Trans, vol. 35, no.2, 1996, pp. 169-176.

[15] L.D. Gibson, “Autonomous control with peer-to-peer I/O networks”, Sensors, vol. 12, no. 9. Sept. 1995, pp. 83-90.

[16] A. Ray, “Introduction to networking for integrated control systems”, IEEE Contr. Syst. Mag., vol. 9, Jan. 1989, pp. 76-79.

[17] G. Schickhuber and O. McCarthy, “Distributed fieldbus and control network systems”, Computing Contr. Eng., vol. 8, no. 1, Feb. 1997, pp. 21-32.

[18] D. Song, T. Divoux, and F. Lepage, “Design of the distributed architecture of a machine-tool using FIP fieldbus”, in Proc. IEEE Int. Conf. Application Specific Systems, Architectures, Processors, Los Alamitos, 1996, pp. 250-260.

[19] G. Cena, C. Demartini, and A. Valenzano, “On the performances of two popular fieldbuses,” in Proc. IEEE Int.Workshop Factory Commun. Syst., Barcelona, Spain, Oct. 1997, pp. 177-186.

[20] J.D. Wheelis, “Process control communications: Token Bus, CSMA/CD, or Token Ring?” ISA Trans., vol. 32, no. 2, July 1993, pp. 193-198.

[21] S. Saad-Bouzefrane and F. Cottet, “A performance analysis of distributed hard real-time applications,” in Proc. IEEE Int. Workshop Factory Commun.Syst., Barcelona, Spain, Oct. 1997, pp. 167-176.

[22] D.R. Wilkie, "The relation between force and velocity in human muscle", J. Physiology, vol. K110, 1950, pp. 248-280.

[23] J.M. Winters, and L. Stark, "Analysis of fundamental human movement patterns through the use on in-depth antagonistic muscle models", IEEE Trans. on Biomed. Engr. vol. BME32, no. 10, 1985.

[24] A. Chu, H. Kazerooni, and A. Zoss, “On the Biomimetic Design of the Berkeley Lower Extremity Exoskeleton (BLEEX)”, IEEE Int. Conf. on Robotics and Automation, Barcelona, Spain, April 2005.

[25] H. Kazerooni, "The extender technology at the University of California, Berkeley," Journal of the Society of Instrument and Control Engineers in Japan, vol. 34, 1995, pp. 291-298.

[26] H. Kazerooni, “The Human Power Amplifier Technology at the University of California, Berkeley”, Journal of Robotics and Autonomous Systems, vol. 19, 1996, pp. 179-187.

[27] K. Amundsen, J. Raade, N. Harding, and H. Kazerooni, “Hybrid Hydraulic-Electric Power Unit for Field and Service Robots,” IEEE IROS, Edmunton, Canada, Aug. 2005.

[28] J. Rose, and J.G. Gamble, *Human Walking*, Second Edition, Williams & Wilkins, Baltimore, 1994, p. 26.

[29] A. Zoss and H. Kazerooni, “On the Mechanical Design of the Berkeley Lower Extemity Exoskeleton,” IEEE IROS, Edmunton Canada, Aug. 2005.

[30] S. Kim, G. Anwar, and H. Kazerooni, “High-speed Communication Network for Controls with Application on the Exoskeleton”, American Control Conference, Boston, June 2004.

[31] S. Kim, and H. Kazerooni, “High-speed Ring-Based Distributed Networked Control System for Real-Time Multivariable Applications,” 2004 IMECE & RD&D Expo, Nov. 2004.

New Techniques in Peripheral Nerve Conduction

Luca Padua[1,2] Pietro Caliandro[1,2] and Erik Stålberg[3]

1 Institute of Neurology, Università Cattolica - Roma, Italy
2 Fondazione Pro Iuventute Don Carlo Gnocchi - Roma, Italy
3 Department of Clinical Neurophysiology, University Hospital - Uppsala, Sweden

INTRODUCTION

The compound motor action potential (CMAP) represents the sum of all activity generated by the motor units within the muscle after nerve stimulation. The CMAP size and shape is determined by the shape characteristics of individual motor unit action potential (MUAP), the position of the motor unit in the muscle, the number of motor units, the range and distribution of conduction velocities (CVs) in the alpha motor fibers, and the distance that the impulse must travel along the nerve.[9] Alpha motor axons have a diameter ranging from 8.3 to 11.8 microns.[8] Conduction velocity of each normal individual axon is proportional to its diameter.[7] In addition, CV depends on membrane characteristics, temperature, and the properties of the myelin sheath.

Since CV is reduced in myelinopathies, its evaluation has clinical utility.[8,11] Conduction velocity usually is measured with the use of a surface electrode (conventional conduction velocity [C-CV]). But C-CV does not optimally define the conduction properties of a nerve because it mainly reflects the fastest-conducting subset of the alpha motor axon population.[1]

Many pathological processes do not affect the nerves uniformly.[10,11] Pathological conditions in the slower conducting subset of axons are usually addressed only indirectly and inferentially; for example, the C-CV is within the normal range, yet there is abnormal amplitude reduction and temporal dispersion of the CMAP.[8] This reduces the sensitivity of C-CV in the evaluation of neuropathies involving mainly slow conducting fibers or, theoretically, neuropathies that do not involve all fibers of a nerve.

A single-fiber electromyography (SFEMG) electrode has been used to increase electrodiagnostic (EDX) sensitivity in the evaluation of nerve conduction block since conduction to individual motor units may be studied.[12] In this technique, random recordings from different sites in the muscle, after repositioning of the electrode, provide the opportunity to study the conduction of a group of individual axons. The purpose of the current study is to evaluate whether, in patients with suspected myelin impairment, it is possible to increase the ability to show abnormal findings in motor nerve conduction studies using an SFEMG electrode when C-CV shows normal findings.

MATERIAL AND METHODS

Conventional motor conduction studies were performed in cases studied by this author and colleagues using an SFEMG needle. This is a specially constructed concentric needle electrode used to record action potentials from individual muscle fibres. The sensitivity of the technique results from the small recording surface (25 microns in diameter).[3] An SFEMG needle electrode is inserted into the muscle and supramaximal stimulation of the nerve is applied at two different sites, both distal and proximal, as in C-CV evaluation. The supramaximal stimulation for both sites was determined earlier by recording conventional CMAPs using surface electrodes

from the muscle. An additional stimulus of 15% above that stimulation strength was used to achieve maximal CMAP amplitude. A high-pass filter of 500 Hz and a low-pass filter of 10,000 Hz were also used.

The method to obtain single-fiber (SF)-CV is approximately the same as that used in the C-CV test, except that the SF-CV procedure verifies that SFEMG responses really are generated by activation of the same axon at distal and proximal stimulation. Using an SFEMG needle electrode, this author and colleagues recorded the potential obtained in response to the supramaximal stimulation of the nerve at the distal site. The criteria used for an acceptable recording were: sharp, spiky, and a fast rise time. It was verified that the needle's position did not change after the first stimulus by applying a second supramaximal stimulus. The potential should have produced the same shape, amplitude, and delay. If the two potentials were different, the position of the needle had changed and the procedure needed to be repeated. The same technique was then applied at the proximal site. In order to ensure that the needle position inside the muscle had not changed, the nerve was stimulated once again at the distal site to verify that the shape, amplitude, and delay of the potential were the same as the first distal stimulation.

To ascertain that the recorded responses obtained after stimulation distally and proximally were the same, a collision technique was used without changing the setting of the recording. A supramaximal stimulus delivered at the distal site elicited a CMAP and an antidromic compound nerve action potential. A second supramaximal stimulus simultaneously applied at the proximal site failed to generate a CMAP since it was blocked by the antidromic volley in each axon. In this author's studies, distal and proximal stimulation pulses were first given with an interstimulus interval (ISI) of 15 ms to generate both distal and proximal responses. The ISI was then changed to 0 ms. In this situation the disappearance of the proximally elicited response was used as proof that the two sites stimulated the same axons and the CV (SF-CV) was then calculated.

Single-fiber-CV was calculated at the onset, or sometimes at a well-identifiable peak of the response. For each nerve, 10 SF-CVs were acquired, moving the SFEMG electrode randomly each time. The low limit of normal SF-CV was defined at 36 m/s because this is the normal value commonly accepted for the slowest CV of alpha motor axons.[4,5,6] Where there was a suspicion of distal segment of the nerve involvement, the distal motor latency through SF-CV test was analyzed. In these cases, normal values obtained through a SFEMG electrode were arbitrarily calculated as the normal values for surface recording plus 30%.

In order to evaluate the normal values (>35m/s), SF-CV was performed in 15 healthy subjects (mean age: 61.8 years, range: 54-70). This author and colleagues studied 22 consecutive patients (9 male, 13 female, mean age 58.9 years, SD 17.86, range 25-82 years) with clinical findings and symptoms suggestive of polyneuropathy, and 9 patients (6 male, 3 female, mean age 56.2 years, SD 15.3, range 35-80 years) with referring symptoms suggestive of nerve entrapment syndromes (5 tarsal tunnel syndromes, 3 ulnar nerve entrapments at the elbow, and 1 peroneal nerve damage at the fibular head), but with normal findings at conventional neurography, including distal latency, CV, amplitude delay, temporal dispersion, F-wave latency, etc. In both the neuropathy and entrapments groups, an extensive clinical and neurophysiological evaluation was performed. Needle EMG was also performed bilaterally on the leg and arm muscles of the neuropathy group.

For each patient in the neuropathy group with pathological findings on conventional tests, one standard-negative nerve (normal at conventional neurography) was selected and studied through SF-CV test. When patients with clinical findings and symptoms suggestive of polyneuropathy showed normal conventional neurophysiological findings, a peroneal nerve was studied by SF-CV test. In the entrapment group, the suspected tract with focal slowing was evaluated through SF-CV tests.

RESULTS

By using a SFEMG needle, the authors studied motor SF-CVs of the peroneal, tibial, and ulnar nerve in 15 healthy subjects. In all subjects, SF-CV was faster than 35 m/s and distal motor latency was normal according to the adopted normal value for all three nerves. Table 1 reports the neurophysiological diagnosis at conventional tests and SF-CV test findings in the neuropathy group.

Table 2 reports conventional and SF-CV tests findings in the entrapment group. In the neuropathy group, 22 standard-negative nerves were evaluated: 9 ulnar, 10 peroneal, and 3 tibial. Fourteen of the 22 (64%) standard-negative nerves presented pathological findings at SF-CV test. Four patients out of the 22 patients in the neuropathy group presented normal findings at conventional tests. Two out of these four patients showed pathological findings at SF-CV test. In eight (89%) out of nine standard-negative entrapment patients abnormal findings during SF-CV test were observed.

In both healthy subjects and patients (in all the sites in which SF-CV was calculated), needle position remained constant. In the first 15 examinations (8 normal subjects and 7 patients), collision technique showed the disappearance of the proximal CMAP when an ISI of 0 ms was used. This result shows that axons recorded after a supramaximal stimulus in the proximal site are the same as those recorded after a supramaximal stimulus in the distal site.

DISCUSSION

Demyelination is neurophysiologically characterized by a reduction in CV of the affected axons. Conventional-CV primarily assesses the fastest axons while an involvement of slow conducting axons remains undetected when measuring CV using conventional neu-

Patient	Age (years)	Sex	Diagnosis at conventional tests	Nerve	Conventional CV (m/s)	No. of pathological SF-CVs	Normal/abnormal SF-CV test
1	74	Female	NF	Peroneal	47.0	0	Normal
2	77	Female	NF	Peroneal	47.0	0	Normal
3	34	Female	Sensory-motor polyneuropathy	Ulnar	66.0	0	Normal
4	74	Female	Sensory-motor multineuropathy	Ulnar	54.0	0	Normal
5	77	Female	Sensory -motor polyneuropathy	Peroneal	64.0	0	Normal
6	82	Female	Motor demyelinating polyneuropathy	Peroneal	37.0	0	Normal
7	82	Female	Motor demyelinating polyneuropathy	Ulnar	49.0	0	Normal
8	40	Female	Motor demyelinating polyneuropathy	Tibial	43.0	1	Abnormal
9	49	Female	Motor demyelinating polyneuropathy	Peroneal	47.0	1	Abnormal
10	63	Female	Sensory-motor polyneuropathy	Peroneal	41.0	1	Abnormal
11	34	Female	Sensory-motor polyneuropathy	Peroneal	44.0	2	Abnormal
12	63	Female	Axonal and demyelinating motor polyneuropathy	Ulnar	42.0	3	Abnormal
13	73	Female	NF	Peroneal	40.0	4	Abnormal
14	25	Male	Axonal sensory polyneuropathy	Ulnar	54.0	0	Normal
15	79	Male	Sensory-motor polyneuropathy	Ulnar	52.0	2	Abnormal
16	57	Male	Demyelinating motor polyneuropathy	Ulnar	57.0	2	Abnormal
17	47	Male	NF	Peroneal	41.0	2	Abnormal
18	64	Male	Sensory-motor polyneuropathy	Ulnar	45.0	3	Abnormal
19	70	Male	Sensory-motor polyneuropathy	Ulnar	42.0	3	Abnormal
20	53	Male	Sensory -motor polyneuropathy	Tibial	41.0	4	Abnormal
21	40	Male	Sensory axonal polyneuropathy	Peroneal	40.0	5	Abnormal
22	40	Male	Sensory axonal polyneuropathy	Tibial	41.0	8	Abnormal

CV = conduction velocity; SF-CV = single-fiber conduction velocity; NF = normal findings.

rography.[11] Changes in slower-conducting axons may affect the shape and dimension of the CMAP; however, there is no reliable method useful to quantify this parameter.

A simulation model was previously used to evaluate the distribution of motor fiber CV in motor nerves with patchy and segmental demyelination. In that study, the authors simulated various degrees of slowing in various axon sample sizes. When the damage involved both small and large axons, the simulations revealed that C-CV was pathological only when severe myelin damage involved a great number axons (AAEM congress, 2004). This is because conventional neurography is heavily dependent on the fastest conducting axons—thus, even if a small portion of axons remains normal, C-CV is within the normal range. The simulations demonstrated that if one could itemize the CMAPs and study the CV of individual axons, the sensitivity in detecting myelin damage would increase.

Recently, a SFEMG electrode has been used to evaluate different portions of the nerve in patients having suspected conduction block.[12] In that study, random recordings from different muscle fibers (moving the electrode in the muscle) provided a rough evaluation of different groups of axons showing minimal conduction block not detectable through conventional surface recordings.

This same technique was adopted to measure CV of a small sample of axons. Using an SFEMG electrode, CV was measured in different groups of individual axons in patients with polyneuropathy and patients with suspected nerve entrapment. A similar technique has

Table 2 Conventional and SF-CV tests findings in the "entrapment" group

Patient	Age (years)	Sex	Diagnosis at conventional tests	Nerve	Conventional CV (m/s)	Conventional DML (ms)	No of pathological sites at SF test	Normal/abnormal SF-CV test
1	35	Female	NF	Peroneal	49.0	_	4	Abnormal
2	58	Female	NF	Tibial	_	3.9	4	Abnormal
3	46	Female	NF	Ulnar	43.0	_	3	Abnormal
4	37	Male	NF	Tibial	_	5.1	6	Abnormal
5	64	Male	NF	Ulnar	50.0	_	1	Abnormal
6	58	Male	NF	Tibial	_	5.8	3	Abnormal
7	54	Male	NF	Ulnar	61.0	_	0	Normal
8	74	Male	NF	Tibial	_	6.2	7	Abnormal
9	80	Male	NF	Tibial	_	5.4	1	Abnormal

CV = conduction velocity; SF-CV = single-fiber conduction velocity; NF = normal findings.

been used in other studies using a concentric needle electrode,[2] but the authors prefer to use a SFEMG needle electrode because of its higher selectivity, which may reflect the CV of a smaller group of axons (or from one axon).

Results from the comparison of SF-CV and C-CV in the studied sample of patients showed that studying nerve function through SFEMG electrode increases neurophysiological sensitivity in demyelinating nerve impairment allowing a neurophysiological diagnosis in 71% patients where conventional studies failed in showing abnormal findings.

SUMMARY

In conclusion, SF-CV evaluation may be useful in detecting early, mild, or partial myelin damage, because it permits the detection of a slowing when conventional tests are normal.

REFERENCES

1. Arasaki K, Iijima M, Nakanishi T. Normal maximal and minimal motor nerve conduction velocities in adults determined by a collision method. Muscle Nerve 1991;14:647-653.
2. Borg J, Grimby L, Hannerz J. Motor neuron firing range, axonal conduction velocity, and muscle fiber histochemistry in neuromuscular diseases. Muscle Nerve 1979;2:423-430.
3. Caliandro P, Stalberg E, Tonali P, Aprile I, Pazzaglia C, Padua L. Single-fiber nerve conduction velocity: simulation and preliminary clinical results. Muscle Nerve 2004;30:528.
4. Cummins KL, Dorfman LJ, Perkel DH. Nerve fiber conduction-velocity distributions. II Estimation based on two compound action potentials. Electroencephalogr Clin Neurophysiol 1979;46:647-658.
5. Dorfman L, Cummins KL, Abraham GS. Conduction velocity distributions of the human median nerve: comparison of methods. Muscle Nerve 1982;5:S148-S153.
6. Dorfman LJ. Computer analysis of compound action potentials recorded with surface electrodes. In: Desmedt JE, editor. Computer-aided electromyography and expert systems. Amsterdam: Elsevier Science Ltd; 1989. p 125-135.
7. Dumitru D, Amato AA, Zwarts MJ. Nerve conduction studies. In: Dumitru D, editor. Electrodiagnostic medicine, 2nd edition. Philadelpia: Hanley and Belfus; 2001. p 169-171.
8. Falck B, Stålberg E. Motor nerve conduction studies: measurement principles and interpretation of findings. J Clin Neurophysiol 1995;12:254-279.
9. Lee RG, Ashby P, White DG, Aguayo AJ. Analysis of motor conduction velocity in the human median nerve by computer simulation of compound muscle action potentials. Electroencephalogr Clin Neurophysiol 1975;39:225-237.
10. Lewis RA, Sumner AJ. The electrodiagnostic distinctions between chronic familial and acquired demyelinative neuropathies. Neurology 1982;32:592-596.
11. McLeod JG, Prineas JW, Walsh JC. The relationship of conduction velocity to pathology in peripheral nerves. In: Desmedt J, editor. New developments in electromyography and clinical neurophysiology. Basel: Karger; 1973. p 249-258.
12. Padua L, Aprile I, D'Amico P, Pauri F, Sabatelli M, Caliandro P, Tonali P. A useful electrophysiological test for diagnosis of minimal conduction block. Clin Neurophysiol 2001;112:1041-1048.

Copper Deficiency Myelopathy

Neeraj Kumar, MD

Assistant Professor
Mayo Clinic College of Medicine
Department of Neurology
Mayo Clinic
Rochester, Minnesota

INTRODUCTION

The hematological manifestations of acquired copper deficiency are well-known and include anemia, neutropenia, and a left shift in granulocytic and erythroid maturation with vacuolated precursors and ringed sideroblasts in the bone marrow.[12,13,61] Only recently have the neurological manifestations of acquired copper deficiency in humans been recognized.4,[15,16,21,26,28-32,34-36,47,48,50,51,61,62] The most common manifestation is a myelopathy presenting with a spastic gait and prominent sensory ataxia.[4,15,21,26,28-32,34-36,50,51,62] Clinical or electrophysiological evidence of an associated peripheral neuropathy is common. Isolated peripheral neuropathy,[16,61] central nervous system (CNS) demyelination,[47,48] and optic neuritis[16] have also been described in association with copper deficiency, but these associations are less well established. Often the cause of the copper deficiency is unclear. The most common abnormality on the spine magnetic resonance imaging (MRI) is increased signal on T2-weighted images involving the dorsal column in the cervical cord.[28] Somatosensory evoked potential and nerve conduction studies suggest impaired central conduction and varying degrees of peripheral neuropathy.[9] Response of the anemia and neutropenia to copper supplementation is prompt and complete.[15,16,31,32,61] With copper supplementation the neurological deterioration may be prevented; improvement, when present, is slight and often subjective.[15,30,32,48,61,62]

NEUROLOGICAL MANIFESTATIONS IN COPPER DEFICIENT ANIMALS

Copper deficiency-associated myelopathy has been described in various animal species.[3,44] Often seen in ruminants, it has been referred to as swayback or enzootic ataxia. The typical distribution of lesions in the spinal cord is greater involvement of the cervical cord with less severe changes in the thoracic and lumbar segments.[44] Wallerian degeneration and demyelination with microcavitation of the white matter of the spinal cord and brainstem may be seen.[3] Menkes disease is the well-known copper deficiency related disease in humans and is due to congenital copper deficiency.[10,39] Comparative neuropathological studies have shown similarity between Menkes disease and swayback.[56] Both are characterized by defects in mitochondrial oxidative metabolism due to decrease in a copper metalloenzyme, cytochrome oxidase.[2,43] Copper-deficient rats have been shown to develop axonal swelling that can reverse with copper supplementation.[17] The activity of cytochrome c oxidase is decreased in various organs in copper-deficient rats.[49]

ROLE OF COPPER IN MAINTAINING THE STRUCTURE AND FUNCTION OF THE NERVOUS SYSTEM

Copper functions as a prosthetic group permitting electron transfer in key enzymatic pathways. It is a component of key metalloenzymes that have a critical role in the structure and function of the nervous system. These include cytochrome c oxidase for electron transport and oxidative phosphorylation in the mitochondrial respiratory chain, copper/zinc superoxide dismutase for antioxidant defense, tyrosinase for melanin synthesis, dopamine beta-hydroxylase for catecholamine biosynthesis, lysyl oxidase for crosslinking of collagen and elastin, peptidylglycine alpha-amidating monooxygenase for neuropeptide and peptide hormone processing, and ceruloplasmin for brain iron homeostasis. Reduction in cytochrome c oxidase activity may be the likely basis for neurological dysfunction associated with the copper deficient state.

CAUSES OF COPPER DEFICIENCY

Copper absorption in humans most likely takes place in the stomach and proximal duodenum.[38] Prompt appearance of ^{64}Cu in the blood after oral administration suggests that most copper absorption occurs from the proximal gut.[55] Copper deficiency following gastric surgery (for peptic ulcer disease or bariatric surgery) is being increasingly recognized.[4,16,19,26,29,30,32,36,51,62] Neurological complications after gastrectomy for ulcer disease or bariatric surgery have been well-recognized, but frequently the cause is not determined.[6,57] However, in a study of 20 patients who had a gastrectomy 4 to 17 years prior, serum copper measurements were comparable with levels seen in control subjects.[54]

Excessive zinc ingestion is a well-recognized cause of copper deficiency.[13,18,22,34,45,50,52,61] In addition to the common use of zinc in the prevention or treatment of common colds and sinusitis, zinc therapy has been used for conditions like acrodermatitis enteropathica, treatment of decubitus ulcers, sickle cell disease, celiac disease, glucagonoma, hepatic encephalopathy, psychosis, memory impairment, diarrhea, myoclonic epilepsy, and acne. Unusual sources of excessive zinc have included a patient who daily consumed an entire tube of a denture cream containing zinc for 5 years,[61] and patients swallowing coins that contained zinc.[18] Zinc causes an upregulation of metallothionein production in the enterocytes.[63] Metallothionein is an intracellular ligand and copper has a higher affinity for metallothionein than zinc. Copper displaces zinc from metallothionein, binds preferentially to the metallothionein, remains in the enterocytes, and is lost in the stools as the intestinal cells are sloughed off.

In Menkes disease, copper deficiency is seen beginning at birth,[39]copper absorption from the gut is impaired,[10] and high levels of copper are seen in duodenal mucosal cells.[11] A defect in enterocyte transport of absorbed copper causes copper accumulation in the intestinal mucosa and resulting hypocupremia. The genetic basis is mutations in the *ATP7A* gene which encodes a P-type adenosine triphosphatase that has multiple copper binding motifs near its amino terminus. Loss of function of this protein results in failure of copper transfer across the gastrointestinal tract, placenta, and blood-brain barrier, with resultant copper deficiency. It is known that mutations in the *ATP7A* gene are responsible for a wide spectrum of manifestations of Menkes disease.[24] Emerging knowledge about copper transport[40,58] may help clarify the etiology of idiopathic hypocupremia. Studies in yeast have shown that reduced copper is transported across the membrane by the high-affinity copper transporter Ctr1 and three different proteins transport copper to cytochrome c oxidase, copper-zinc superoxide dismutase, and the post-Golgi compartment for insertion into a multicopper oxidase essential for high-affinity iron uptake. The copper transporter Ctr1 is the primary avenue for copper uptake in mammalian cells and provides an essential function in mammalian embryonic development.[37]

Copper deficiency may occur in premature infants and low birthweight infants.[1] Because of copper's ubiquitous distribution and low daily requirement, acquired dietary copper deficiency is rare.[60] It may occur in malnourished infants,[7] nephrotic syndrome,[5] and enteropathies associated with malabsorption.[8,35] Copper deficiency may be a complication of prolonged total parenteral nutrition (TPN),[59] particularly when copper supplementation in TPN is withheld due of cholestasis.[14] Enteral feeding with inadequate copper has also been known to result in copper deficiency.[42]

CLINICAL FEATURES, NEUROPHYSIOLOGY, AND NEUROIMAGING IN COPPER DEFICIENCY MYELOPATHY

The neurological manifestation of acquired copper deficiency is typically that of gait difficulty primarily due to severe sensory ataxia. The sensory ataxia is due to dorsal column dysfunction. Clinical or electrophysiological evidence of a peripheral neuropathy is often present. Involvement of the peripheral nervous system is not the predominant reason for the sensory ataxia. The MRI and evoked potential studies provide additional evidence of posterior column dysfunction. Other reported electrophysiological abnormalities noted in patients with copper deficiency and neurological manifestations include prolonged visual evoked potentials,[47] and impaired central conduction on transcranial magnetic stimulation.[51] The most consistent finding on an MRI of the spine is increased signal on T2-weighted images involving the dorsal columns (Figure1, A, B). The cervical cord is most commonly involved and contrast enhancement is not present. Follow-up imaging may show resolution of the dorsal column signal change with improvement in serum copper.[28]

ASSOCIATED HYPERZINCEMIA

An elevated serum zinc level in the absence of exogenous zinc ingestion is commonly seen in associated hyperzincemia.[15,21,32,48,61]

The hyperzincemia (as assessed by increased serum zinc or urinary zinc excretion) may persist or increase despite correction of the copper deficient state.[15,21,32,48] The significance of the associated hyperzincemia seen in the absence of exogenous zinc ingestion is unclear.[20,27] Also uncertain is the significance of increased urinary zinc excretion without elevation of the plasma zinc level.[35,36] It has been suggested that the copper deficiency may result from a zinc overload syndrome.[21] A metabolic abnormality resulting in increased zinc absorption or decreased intestinal excretion has been proposed. Since the syndrome of myeloneuropathy has been described with hypocupremia and normal zinc levels,[29,30,32,35,36,51] it is unlikely that hyperzincemia is causative. There are no definite reports of neurologic toxicity due to hyperzincemia without hypocupremia in animals or humans. Elevated zinc levels have also been described as a heritable anomaly with no clinical manifestations.[53] Chronically administered high doses of oral zinc have been used in patients with Wilson's disease without the development of neurological complications. The hyperzincemia seen in some patients with neurological manifestations and copper deficiency is probably a secondary feature associated with the hypocupremia.

ASSOCIATED VITAMIN B_{12} DEFICIENCY

A prior history of vitamin B_{12} deficiency may be present with copper deficiency. Not infrequently these patients have had a prior history of gastric surgery. The vitamin B_{12} levels is generally normal at the time the copper deficient state was diagnosed. The myelopathy of copper deficiency closely mimics the subacute combined degeneration of vitamin B_{12} deficiency.[32] Copper and vitamin B_{12} deficiency may coexist.[32,61] Patients may be given vitamin B_{12} despite normal serum vitamin B_{12} levels.[51] Similar spine MRI appearance can be seen in patients with vitamin B_{12} deficiency.

ASSOCIATED HEMATOLOGIC MANIFESTATIONS

There are several hematologic manifestations associated with copper deficiency. A history of anemia or leukopenia, or anemia or leukopenia at presentation is commonly present. It is becoming increasingly more recognizable that hematological manifestations may not accompany the neurological syndrome.[30,32-34] The hematological hallmark of copper deficiency is anemia and neutropenia.[12,22,42] The anemia may be microcytic,[22,45] macrocytic,[16,61] or normocytic.[61] Thrombocytopenia and resulting pancytopenia is relatively rare.[14,59] It has been suggested that a prolonged copper-deficient state may be necessary for the development of thrombocytopenia.[42]

Typical bone marrow findings include a left shift in granulocytic and erythroid maturation with cytoplasmic vacuolization in erythroid and myeloid precursors and the presence of ringed sideroblasts (Figure 1, C-E).[12,47,61] Hemosiderin containing plasma cells may be present (Figure 1, C-E).[12,16] The bone marrow findings are not pathognomic but are highly characteristic and there are reports of patients in whom diagnosis of the copper deficient state was first suggested by the bone marrow findings.[61] Patients may be given a diagnosis of sideroblastic anemia or myelodysplastic syndrome.[13,16,25,31,61]

Copper containing enzymes likely play a role in cell differentiation and proliferation in the bone marrow. Impaired erythroid and myeloid maturation and reduced erythrocyte and neutrophil lifespans are the likely reasons for the anemia and neutropenia.

TREATMENT OF COPPER DEFICIENCY

There have been no studies that address the most appropriate dose, duration, route, and form of copper supplementation. There is little information available on human copper stores. It has been suggested that serum copper may be inadequate for assessing total body copper stores and activity of copper enzymes like erythrocyte superoxide dismutase and platelet or leukocyte cytochrome c oxidase may be a better indicator of metabolically active copper stores.[41]

In patients with zinc-induced copper deficiency discontinuing the zinc may suffice and no additional copper supplementation may be required.[61] Prolonged oral therapy at times may not result in improvement; parenteral thereapy may be required and it has been suggested that elimination of excess zinc may be slow and until such elimination occurs, the intestinal absorption of copper may be blocked.[22] Some have employed initial parenteral administration followed by oral administration.[16,50]

Despite a suspected absorption defect, oral copper supplementation is generally the preferred route of supplementation. Copper supplements may not be adequately absorbed when administered through a jejunostomy tube, necessitating parenteral therapy.[23] Studies in yeast have shown that the copper transport pathways are high-affinity pathways, active in conditions of low copper concentration, and increasing the concentration of copper may result in the pathways being bypassed.[58] This may explain why in a majority of this authors' patients normal serum copper levels were achieved by increasing the amount of copper ingested. In most cases oral administration of 2 mg of elemental copper a day seems to suffice. A comparable dose of elemental copper may be given intravenously. Doses up to 9 mg/day orally have been used.[4,16,21] Commonly used copper salts include copper gluconate[4] and copper chloride.[16] The bioavailability of oral copper gluconate may be limited.[46]

In this author's recent practice, 6 mg of elemental copper was orally administered daily for the first week, 4 mg a day for the second week, and 2 mg a day thereafter. Periodic assessment of serum copper is essential to determine adequacy of replacement and to decide on the most appropriate long-term administration strategy. Because of the need for long-term replacement, parenteral therapy is not preferred and is generally not required. If required a daily

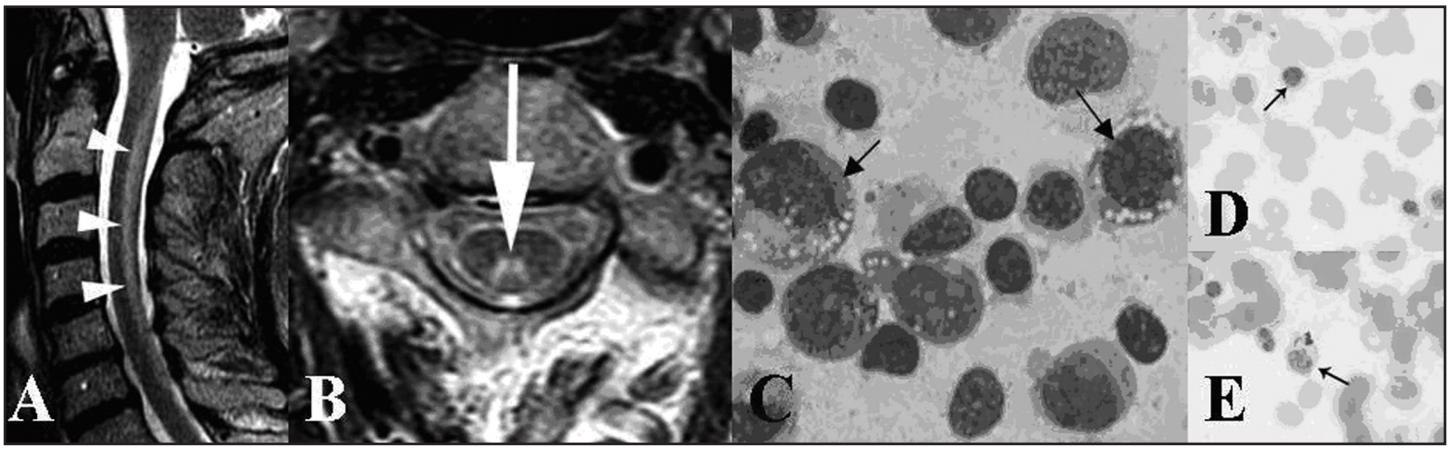

Figure 1 A and B Sagittal (A) and axial (B) T2-weighted magnetic resonance images in a patient with copper deficiency myelopathy showing increased signal in the paramedian aspect of the dorsal cervical cord. **C, D, and E** Bone marrow studies from patients with copper deficiency myelopathy showing showing vacuolated myeloid precursors (C), ringed sideroblast (D), and iron containing plasma cell (E).

dose of 2 mg of elemental copper may be administered intravenously for 5 days and periodically thereafter.

Response of the hematological parameters (including bone marrow findings) is prompt and often complete.[13-16,45,59,61] Hematological recovery may be accompanied by reticulocytosis.[15,64] Transient improvement with hematopoietic growth factors may occur even if copper deficiency is the cause of the hematological manifestations.[16,31] Recovery of neurological signs and symptoms seen in association with copper deficiency is variable. Improvement in neurological symptoms is generally absent though progression is typically halted.[15,30,32,48,61,62] A relapse in the copper-deficient state may not be necessarily accompanied by neurological deterioration.[48] Improvement when present is often subjective and preferentially involves sensory symptoms.[36,48,51] There are some reports of definite improvement in the neurological deficits,[21,47,50] nerve conduction studies,[50] evoked potential studies,[34] and MRI T2 cord signal change[28] with normalization of serum copper.

CONCLUSIONS

The most common neurological manifestation of acquired copper deficiency is that of a myelopathy presenting with a spastic gait and prominent sensory ataxia. The neurological syndrome due to acquired copper deficiency may be present without the more commonly reported hematological manifestations. A peripheral neuropathy of variable severity is commonly associated. Somatosensory evoked potential studies may show delay in central conduction. Spinal cord MRI in patients with copper deficiency myelopathy may show increased signal on T2-weighted images, most commonly in the paramedian cervical cord.

Identifiable causes of acquired copper deficiency include a prior history of gastric surgery, excessive zinc ingestion, parenteral alimentation without adequate supplementation, and malabsorption. Often the cause of the copper deficiency is unclear. Hyperzincemia may be present even in the absence of exogenous zinc ingestion.

It is unclear which patients may develop copper deficiency after gastric surgery and whether or not routine screening and supplementation should be considered as is commonly done for vitamin B_{12} deficiency. Given the increasing rates of bariatric surgery, this is a particularly pertinent issue. It might be decades before the copper-deficient state manifests. The role of the commonly observed hyperzincemia in the absence of exogenous zinc ingestion is unclear. The postulated reduction in copper absorption by oral iron therapy is not well established. The association between copper deficiency and CNS demyelination, isolated peripheral neuropathy, and optic neuritis requires further study. Studies are needed to determine the best dose, route, and duration of copper therapy. Further understanding of copper transport and trafficking may provide insights into the cause of copper deficiency in those with idiopathic hypocupremia.

The clinical features and neuroimaging is very similar to the subacute combined degeneration seen in patients with vitamin B_{12} deficiency. Copper and vitamin B_{12} deficiency may coexist. Continued neurological deterioration in patients with a history of vitamin B_{12} deficiency related myelopathy who have a normal

vitamin B_{12} level on vitamin B_{12} replacement should be evaluated for copper deficiency. Early recognition and prompt treatment may prevent significant neurologic morbidity.

Response of the anemia and neutropenia to copper supplementation is prompt and complete. With copper supplementation the neurological deterioration may be prevented. Improvement when present is often subjective and preferentially involves sensory symptoms.

Estimation of serum copper levels should be a part of the work up in patients with a myelopathy or myeloneuropathy particularly so in patients with a high risk of developing copper deficiency. The presence of unexplained cytopenia in association with neurological manifestations should prompt clinicians to look for copper deficiency.

ADDENDUM

Two additional patients with copper deficiency myelopathy and prior gastric surgery have recently been described (1. Prodan CI, Bottomley SS, Holland NR, Lind SE. Relapsing hypocupraemic myelopathy requiring high-dose oral copper replacement. J Neurol Neurosurg Psychiatry 2006;77:1092-1093. 2. Tan JC, Burns DL, Jones HR. Severe ataxia, myelopathy, and peripheral neuropathy due to acquired copper deficiency in a patient with history of gastrectomy. JPEN J Parenter Enteral Nutr. 2006;30:446-450.) . Copper deficiency myelopathy has also been reported in association with parenteral zinc supplementation during hemodialysis (Yaldizli O, Johansson U, Gizewski ER, Maschke M. Copper deficiency myelopathy induced by repetitive parenteral zinc supplementation during chronic hemodialysis. J Neurol 10.1007/s00415-006-0259-z Published online on 13 September 2006.).

Also noteworthy is a recent report of three patients who presented with asymmetric lower motor neuron weakness, minimal sensory manifestations, and electrodiagnostic evidence of diffuse denervation. Two of these had a history of gastrointestinal surgery (Weihl CC, Lopate G. Motor neuron disease associated with copper deficiency. Muscle Nerve 10.1002/mus.20631 Published online on 23 Aug 2006.).

Interested readers are directed to a recent review that describes 25 patients with copper deficiency myelopathy (Kumar N. Copper deficiency myelopathy: "Human Swayback". Mayo Clin Proc 2006;81:1371-1384.).

REFERENCES

1. Al-Rashid RA, Spangler J. Neonatal copper deficiency. New Engl J Med 1971;285:841-843.
2. Alleyne T, Joseph J, Lalla A, Sampson V, Adogwa A. Cytochrome-c oxidase isolated from the brain of swayback-diseased sheep display unusual structure and uncharacteristic kinetics. Mol Chem Neuropathol 1998;34:233-247.
3. Barlow RM. Further observations on swayback. Part I. Transitional pathology. J Comp Pathol 1963;73:51-60.
4. Bartner R, Will M, Conrad J, Engelhardt A, Schwarz-Eywill M. Kupfermangel als seltene Ursache von Panzytopenie, Arthralgien und Gangstorungen. Med Klin 2005;100:497-501.
5. Cartwright GE, Gubler CJ, Wintrobe MM. Studies on copper metabolism. XI. Copper and iron metabolism in the nephrotic syndrome. J Clin Invest 1954;33:685-698.
6. Chang CG, Adams-Huet B, Provost DA. Acute post-gastric reduction surgery (APGARS) neuropathy. Obes Surg 2004;14:182-189.
7. Cordano A, Baertl JM, Graham GG. Copper deficiency in infancy. Pediatrics 1964;34:324-336.
8. Cordano A, Graham GG. Copper deficiency complicating severe chronic malabsorption. Pediatrics 1966;38:596-604.
9. Crum BA, Kumar N. Electrophysiologic findings in copper deficiency myeloneuropathy. Neurology 2005;64:A123.
10. Danks DM, Campbell PE, Stevens BJ, Mayne V, Cartwright E. Menkes's kinky hair syndrome. An inherited defect in copper absorption with widespread effects. Pediatrics 1972;50:188-201.
11. Danks DM, Cartwright E, Stevens BJ, Townley RR. Menkes' kinky hair disease: further definition of the defect in copper transport. Science 1973;179:1140-1142.
12. Dunlap WM, James GW 3rd, Hume DM. Anemia and neutropenia caused by copper deficiency. Ann Intern Med 1974;80:470-476.
13. Fiske DN, McCoy HE 3rd, Kitchens CS. Zinc-induced sideroblastic anemia: report of a case, review of the literature, and description of the hematologic syndrome. Am J Hematol 1994;46:147-150.
14. Fuhrman MP, Herrmann V, Masidonski P, Eby C. Pancytopenia after removal of copper from total parenteral nutrition. JPEN J Parenter Enteral Nutr 2000;24:361-366.
15. Greenberg SA, Briemberg HR. A neurological and hematological syndrome associated with zinc excess and copper deficiency. J Neurol 2004;251:111-114.
16. Gregg XT, Reddy V, Prchal JT. Copper deficiency masquerading as myelodysplastic syndrome. Blood 2002;100:1493-1495.
17. Hartmann HA, Evenson MA. Deficiency of copper can cause neuronal degeneration. Med Hypotheses 1992;38:75-85.
18. Hassan HA, Netchvolodoff C, Raufman JP. Zinc-induced copper deficiency in a coin swallower. Am J Gastroenterol 2000;95:2975-2977.
19. Hayton BA, Broome HE, Lilenbaum RC. Copper deficiency-induced anemia and neutropenia secondary to intestinal malabsorption. Am J Hematol 1995;48:45-47.
20. Hedera P, Brewer GJ. Myeloneuropathy due to copper deficiency or zinc excess? Arch Neurol 2004;61:605.
21. Hedera P, Fink JK, Bockenstedt PL, Brewer GJ. Myelopolyneuropathy and pancytopenia due to copper deficiency and high zinc levels of unknown origin: further support for existence of a new zinc overload syndrome. Arch Neurol 2003;60:1303-1306.
22. Hoffman HN 2nd, Phyliky RL, Fleming CR. Zinc-induced copper deficiency. Gastroenterology 1988;94:508-512.
23. Jayakumar S, Micallef-Eynaud PD, Lyon TD, Cramb R, Jilaihawi AN, Prakash D. Acquired copper deficiency following prolonged jejunostomy feeds. Ann Clin Biochem 2005;42:227-231.

24. Kaler SG. Metabolic and molecular bases of Menkes disease and occipital horn syndrome. Pediatr Dev Pathol 1998;1:85-98.
25. Kumar A, Jazieh AR. Case report of sideroblastic anemia caused by ingestion of coins. Am J Hematol 2001;66:126-129.
26. Kumar N, Ahlskog JE, Gross JB Jr. Acquired hypocupremia after gastric surgery. Clin Gastroenterol Hepatol 2004;2:1074-1079.
27. Kumar N, Ahlskog JE. Myeloneuropathy due to copper deficiency or zinc excess? Arch Neurol 2004;61:604-605.
28. Kumar N, Ahlskog JE, Klein CJ, Port JD. Imaging features of copper deficiency myelopathy: a study of 25 cases. Neuroradiology 2006;48:78-83.
29. Kumar N, Crum B, Petersen RC, Vernino S, Ahlskog JE. Copper deficiency myelopathy. Arch Neurol 2004;61:762-766.
30. Kumar N, Crum BC, Ahlskog JE. Copper deficiency myelopathy. Neurology 2005;64:A419.
31. Kumar N, Elliott MA, Hoyer JD, Harper CM Jr, Ahlskog JE, Phyliky RL. "Myelodysplasia," myeloneuropathy, and copper deficiency. Mayo Clin Proc 2005;80:943-946.
32. Kumar N, Gross JB Jr, Ahlskog JE. Copper deficiency myelopathy produces a clinical picture like subacute combined degeneration. Neurology 2004;63:33-39.
33. Kumar N, Gross JB Jr, Ahlskog JE. Myelopathy due to copper deficiency. Neurology 2004:1656.
34. Kumar N, Gross JB Jr, Ahlskog JE. Myelopathy due to copper deficiency. Neurology 2003;61:273-274.
35. Kumar N, Low PA. Myeloneuropathy and anemia due to copper malabsorption. J Neurol 2004;251:747-749.
36. Kumar N, McEvoy KM, Ahlskog JE. Myelopathy due to copper deficiency following gastrointestinal surgery. Arch Neurol 2003;60:1782-1785.
37. Kuo YM, Zhou B, Cosco D, Gitschier J. The copper transporter CTR1 provides an essential function in mammalian embryonic development. Proc Natl Acad Sci U S A 2001;98:6836-6841.
38. Mason KE. A conspectus of research on copper metabolism and requirements of man. J Nutr 1979;109:1979-2066.
39. Menkes JH, Alter M, Steigleder GK, Weakley DR, Sung JH. A sex-linked recessive disorder with retardation of growth, peculiar hair, and focal cerebral and cerebellar degeneration. Pediatrics 1962;29:764-779.
40. Mercer JF, Llanos RM. Molecular and cellular aspects of copper transport in developing mammals. J Nutr 2003;133:1481S-1484S.
41. Milne DB. Assessment of copper nutritional status. Clin Chem 1994;40:1479-1484.
42. Nagano T, Toyoda T, Tanabe H, Nagato T, Tsuchida T, Kitamura A, Kasai G. Clinical features of hematological disorders caused by copper deficiency during long-term enteral nutrition. Intern Med 2005;44:554-559.
43. Pedespan JM, Jouaville LS, Cances C, Letellier T, Malgat M, Guiraud P, Coquet M, Vernhet I, Lacombe D, Mazat JP. Menkes disease: study of the mitochondrial respiratory chain in three cases. Eur J Paediatr Neurol 1999;3:167-170.
44. Penrith ML, Tustin RC, Thornton DJ, Burdett PD. Swayback in a blesbok (Damaliscus dorcas phillipsi) and a black wildebeest (Connochaetes gnou). J S Afr Vet Assoc 1996;67:93-96.
45. Prasad AS, Brewer GJ, Schoomaker EB, Rabbani P. Hypocupremia induced by zinc therapy in adults. JAMA 1978;240:2166-2168.
46. Pratt WB, Omdahl JL, Sorenson JR. Lack of effects of copper gluconate supplementation. Am J Clin Nutr 1985;42:681-682.
47. Prodan CI, Holland NR. CNS demyelination from zinc toxicity? Neurology 2000;54:1705-1706.
48. Prodan CI, Holland NR, Wisdom PJ, Burstein SA, Bottomley SS. CNS demyelination associated with copper deficiency and hyperzincemia. Neurology 2002;59:1453-1456.
49. Prohaska JR. Changes in tissue growth, concentrations of copper, iron, cytochrome oxidase and superoxide dismutase subsequent to dietary or genetic copper deficiency in mice. J Nutr 1983;113:2048-2058.
50. Rowin J, Lewis SL. Copper deficiency myeloneuropathy and pancytopenia secondary to overuse of zinc supplementation. J Neurol Neurosurg Psychiatry 2005;76:750-751.
51. Schleper B, Stuerenburg HJ. Copper deficiency-associated myelopathy in a 46-year-old woman. J Neurol 2001;248:705-706.
52. Simon SR, Branda RF, Tindle BF, Burns SL. Copper deficiency and sideroblastic anemia associated with zinc ingestion. Am J Hematol 1988;28:181-183.
53. Smith JC, Zeller JA, Brown ED, Ong SC. Elevated plasma zinc: a heritable anomaly. Science 1976;193:496-498.
54. Stael von Holstein C, Ibrahimbegovic E, Walther B, Akesson B. Nutrient intake and biochemical markers of nutritional status during long-term follow-up after total and partial gastrectomy. Eur J Clin Nutr 1992;46:265-272.
55. Sternlier I, Morell AG, Bauer CD, Combes B, De Bobes-Sternberg S, Schein-Berg IH. Detection of the heterozygous carrier of the Wilson's disease gene. J Clin Invest 1961;40:707-715.
56. Tan N, Urich H. Menkes' disease and swayback. A comparative study of two copper deficiency syndromes. J Neurol Sci 1983;62:95-113.
57. Thaisetthawatkul P, Collazo-Clavell ML, Sarr MG, Norell JE, Dyck PJ. A controlled study of peripheral neuropathy after bariatric surgery. Neurology 2004;63:1462-1470.
58. Valentine JS, Gralla EB. Delivering copper inside yeast and human cells. Science 1997;278:817-818.
59. Wasa M, Satani M, Tanano H, Nezu R, Takagi Y, Okada A. Copper deficiency with pancytopenia during total parenteral nutrition. JPEN J Parenter Enteral Nutr 1994;18:190-192.
60. Williams DM. Copper deficiency in humans. Semin Hematol 1983;20:118-128.
61. Willis MS, Monaghan SA, Miller ML, McKenna RW, Perkins WD, Levinson BS, Bhushan V, Kroft SH. Zinc-induced copper deficiency: a report of three cases initially recognized on bone marrow examination. Am J Clin Pathol 2005;123:125-131.
62. Wu J, Ricker M, Muench J. Copper deficiency as cause of unexplained hematologic and neurologic deficits in patient with prior gastrointestinal surgery. J Am Board Fam Med 2006;19:191-194.
63. Yuzbasiyan-Gurkan V, Grider A, Nostrant T, Cousins RJ, Brewer GJ. Treatment of Wilson's disease with zinc: X. Intestinal metallothionein induction. J Lab Clin Med 1992;120:380-386.
64. Zidar BL, Shadduck RK, Zeigler Z, Winkelstein A. Observations on the anemia and neutropenia of human copper deficiency. Am J Hematol 1977;3:177-185.

Neuromuscular Disorders and Techniques: Novel Observations and Fresh Looks

CME SELF-ASSESSMENT TEST

Select the ONE best answer for each question.

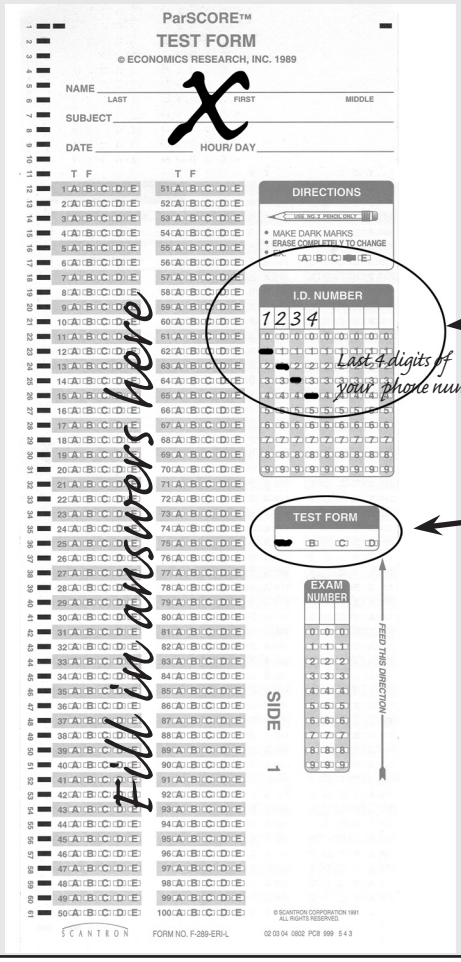

Instructions for filling out your parSCORE sheet

On the right-hand side of the parSCORE sheet, you will need to fill in the following:

Under ID number, please write out and fill in the last 4 digits of your phone number. Be sure to start in the first box on the left (as shown).

Under Test Form, please fill in "A".

Leave the completed form at the table outside your session.

1. In hereditary sensory and autonomic neuropathy type I (HSAN I):
   A. All modes of sensation are equally impaired.
   B. Trunkal regions are seldom involved.
   C. Motor signs are uncommon.
   D. Motor nerve conduction velocities are normal.
   E. Sensory action potentials are paradoxically retained.

2. Which of the following IS **NOT** a prominent feature of HSAN II?
   A. Mutilating acropathy.
   B. Loss of muscle stretch reflexes.
   C. Overt motor weakness.
   D. Normal or slightly slowed motor conduction velocities.
   E. Demyelination of peripheral sensory axons, affecting all fiber sizes.

3. Early loss of pain awareness IS **NOT** a feature of which of the following neuropathic conditions?
   A. Analphalipoproteinemia.
   B. Abetalipoproteinemia.
   C. Fabry disease.
   D. Hansen disease.
   E. Hereditary coproporphyria.

4. In HSAN II:
   A. Inheritance is autosomal recessive.
   B. Onset of symptoms is usually between 15-50 years.
   C. Acropathy affects only the feet.
   D. The course is rapidly progressive.
   E. Lancinating pain is not a feature.

5. Body-wide loss of the appreciation of pain is:
   A. Usually a genetic disorder.
   B. Due to damage to thin-fiber peripheral axons.
   C. Never physiological.
   D. Likely due to a disorder of the central processor for pain perception.
   E. Associated with bilateral impairment of cortical discriminatory sensation.

6. What statements **best** describe the characteristics of the small fiber system?
   A. It comprises A-delta or Group III fibers and C or Group IV fibers.
   B. The fibers are activated by mechanical, thermal, and chemical irritation.
   C. Nociceptors have a peripheral neurosecretory function that causes vasodilatation, an action that can balance the vasoconstrictive effects of the sympathetic fibers.
   D. These fibers can be sensitized.
   E. All of above.

7. Neurogenic inflammation is a cascade of chemical releases that involves
   which of the following events?
   A. Histamine, bradykinin, and prostaglandin are released from the primary afferent fiber.
   B. Excess peripheral release of substance P (SP), calcitonin gene-related peptide (CGRP), and somatostatin from the primary afferent fiber.
   C. Excess central release of SP, CGRP, and somatostatin from the primary afferent.
   D. The destruction of nerve fibers by loss of blood supply
   E. All of the above.

8. What is the current hypothesis about the mechanism behind the unusual remote referral patterns of pain associated with myofascial trigger points?
   A. The referral pattern is evidence of psychological disturbance.
   B. A subtle radiculopathy is the real cause of pain, not a trigger point.
   C. The opening of previously ineffective connections in the dorsal horn that
   develops with sustained noxious input.
   D. Peripheral sensitization.
   E. Neurogenic inflammation.

9. Which of the following substances is significantly decreased in an active trigger
   point following a local twitch response?
   A. SP, tumor necrosis factor (TNF)-alpha.
   B. SP, calcitonin gene-related peptide.
   C. Bradykinin, TNF-alpha.
   D. Serotonin, SP.
   E. Norepinephrine, bradykinin.

10. Peripheral sensitization is fueled by all of the following mechanisms **EXCEPT**:
    A. Expression of sodium channels that more rapidly repolarized.
    B. Lowered pH in the periphery.
    C. Elevated bradykinin in the periphery.
    D. Lower SP levels in the periphery.
    E. Elevated serotonin in the periphery.

11. All of the following are true regarding copper deficiency myelopathy **EXCEPT**:
    A. Gait difficulty is primarily due to lower limb weakness.
    B. Central slowing may be seen on somatosensory evoked potential studies.
    C. An increased signal involving the dorsal column in the cervical cord may be seen on T2-weighted magnetic resonance imaging (MRI).
    D. Clinical or electrophysiologic evidence of a peripheral neuropathy is often present.
    E. Copper deficiency myelopathy may be seen without hematologic manifestations of copper deficiency.

12. Copper deficiency can result from:
    A. Malnutrition.
    B. Malabsorption.
    C. Excessive zinc ingestion.
    D. A prior history of gastric surgery.
    E. All of the above.

13. Which of the following is **NOT** true about the laboratory abnormalities in patients with copper deficiency myelopathy?
    A. Anemia or neutropenia are often present.
    B. Vitamin B12 deficiency may coexist with copper deficiency.
    C. An elevated serum zinc is seen only in the presence of exogenous ingestion.
    D. Bone marrow evaluation may show a left shift in granulocytic and erythroid maturation.
    E. Serum copper estimation is more reliable than serum ceruloplasmin in making the diagnosis of copper deficiency.

14. Copper containing metalloenzymes include:
    A. Cytochrome c oxidase (oxidative phosphorylation).
    B. Dopamine beta-hydroxylase (catecholamine biosynthesis).
    C. Superoxide dismutase (antioxidant defense).
    D. Peptidylglycine alpha-amidating monooxygenase (neuropeptide processing).
    E. All of the above.

15. All of the following are true regarding copper deficiency myelopathy **EXCEPT**:
    A. Often the cause of copper deficiency is not evident
    B. Even before its description in humans, copper deficiency myelopathy had been documented in various animal species
    C. Oral copper administration is the preferred route for correction of the copper deficiency
    D. Response of the associated hematological derangement is generally not seen
    E. The typical neurological outcome is prevention of worsening of the myelopathy

Neuromuscular Disorders and Techniques: Novel Observations and Fresh Looks

EVALUATION

Select ANY of the answers that indicate your opinions.

Your input is needed to critique our courses and to ensure that we use the best faculty instructors and provide the best course options in future years. Make additional comments or list suggested topics or faculty for future courses on the comment form provided at the end of this handout.

16. How would you rate the quality of instruction received during Dr. Pryse-Phillips's presentation?
    A. Best possible.
    B. Good.
    C. Average.
    D. Poor.
    E. Worst possible.

17. Select any item(s), that, if changed, would have appreciably improved Dr. Pryse-Phillips's presentation:
    A. Quality of slides.
    B. Quality of handout.
    C. Amount of clinically relevant information in the presentation.
    D. Amount of scientific content in the presentation.
    E. Other: please explain on the comment form at the back of this handout.

18. Did you perceive any commercial bias in Dr. Pryse-Phillips's presentation?
    A. Yes.
    B. No.

19. How would you rate the quality of instruction received during Dr. Shah's presentation?
    A. Best possible.
    B. Good.
    C. Average.
    D. Poor.
    E. Worst possible.

20. Select any item(s), that, if changed, would have appreciably improved Dr. Shahs presentation:
    A. Quality of slides.
    B. Quality of handout.
    C. Amount of clinically relevant information in the presentation.
    D. Amount of scientific content in the presentation.
    E. Other: please explain on the comment page at the back of this handout.

21. Did you perceive any commercial bias in Dr. Shah's presentation?
    A. Yes.
    B. No.

22. How would you rate the quality of instruction received during Dr. Lennon's presentation?
    A. Best possible.
    B. Good.
    C. Average.
    D. Poor.
    E. Worst possible.

23. Select any item(s), that, if changed, would have appreciably improved Dr. Lennon's presentation:
    A. Quality of slides.
    B. Quality of handout.
    C. Amount of clinically relevant information in the presentation.
    D. Amount of scientific content in the presentation.
    E. Other: please explain on the comment page at the back of this handout.

24. Did you perceive any commercial bias in Dr. Lennons presentation?
    A. Yes.
    B. No.

25. How would you rate the quality of instruction received during Dr. Kazerooni's presentation?
    A. Best possible.
    B. Good.
    C. Average.
    D. Poor.
    E. Worst possible.

26. Select any item(s), that, if changed, would have appreciably improved Dr. Kazeroonis presentation:
    A. Quality of slides.
    B. Quality of handout.
    C. Amount of clinically relevant information in the presentation.
    D. Amount of scientific content in the presentation.
    E. Other: please explain on the comment page at the back of this handout.

27. Did you perceive any commercial bias in Dr. Kazerooni's presentation?
    A. Yes.
    B. No.

28. How would you rate the quality of instruction received during Dr. Kumar's presentation?
    A. Best possible.
    B. Good.
    C. Average.
    D. Poor.
    E. Worst possible.

29. Select any item(s), that, if changed, would have appreciably improved Dr. Kumar's presentation:
    A. Quality of slides.
    B. Quality of handout.
    C. Amount of clinically relevant information in the presentation.
    D. Amount of scientific content in the presentation.
    E. Other: please explain on the comment page at the back of this handout.

30. Did you perceive any commercial bias in Dr. Kumar's presentation?
    A. Yes.
    B. No.

31. As a result of your attendance at this educational session, did you learn anything that will improve the care of your patients?
    A. Yes, substantially.
    B. Yes, somewhat.
    C. Not sure.
    D. Probably not.
    E. This session was not applicable to my patients.

32. Do you feel that the information presented in this session was based on the best evidence available?
    A. Yes.
    B. No: please explain on the comment page at the back of this handout.

33. Select ALL items where improvement was needed.
    A. The accuracy of advance descriptions of this course.
    B. The specific topics selected for presentation.
    C. The number of speakers in this course.
    D. The amount of time allotted for discussion in this course.
    E. Other: please add other areas and outline specific recommendations for areas needing improvement on the comment page at the back of this handout.

34. I plan to attend the 2007 AANEM Annual Meeting in Phoenix, AZ October 17-20.
    A. Yes, definitely.
    B. No, definitely.
    C. Will wait to see the program content.
    D. Will wait to see if budget allows my attendance.

35. We would like the AANEM Annual Meeting to be one of your "must attend" meetings each year. In order to do this, we would have to do what to make it happen? Please explain on the comment page at the back of this handout.

36. If you are a member of the AANEM, what would you rate as the most valuable benefit of your membership?
    A. My subscription to the journal *Muscle & Nerve*.
    B. Receiving free educational materials such as the *Muscle & Nerve* Invited Reviews and the AANEM Resource CD.
    C. The availability of CME opportunities.
    D Member discounts on AANEM CME products and services.
    E. AANEM's advocacy work on issues that impact my profession.

37. In 2006, the AANEM distributed 6 bound copies of the *Muscle & Nerve* Invited Reviews. How would you rate this new member benefit?
    A. Very valuable.
    B. Somewhat valuable.
    C. Not very valuable.
    D. I do not receive this since I am not an AANEM member.
    E. Other: please explain on the comment page at the back of this handout.

38. When you receive the bound copies of the *Muscle & Nerve* Invited Reviews, you can visit the AANEM website and complete CME questions to receive a certificate at no charge. Have you utilized this new service?
    A. Yes, I have completed CME for the Invited Reviews online and found the system easy to utilize.
    B. Yes, I have completed CME for the Invited Reviews online, but found the system difficult to utilize.
    C. No, I have not utilized this service because I was unaware it was available.
    D. No, I have not utilized it although I was aware of its availability: please explain on the comment page at the back of this handout.
    E. Other: please explain on the comment page at the back of this handout.

39. In 2006, the AANEM added Online Case Studies to the website which are also available for CME credit. How would you rate this new member benefit?
    A. Very valuable.
    B. Somewhat valuable.
    C. Not very valuable.
    D. I was not aware that this was available on the AANEM website.
    E. Other: please explain on the comment page at the back of this handout.

45. The AANEM has recently launched new Marketing Slides on the website that can assist EDX physicians in marketing to referral sources. How would you rate this member benefit?
    A. Very valuable.
    B. Somewhat valuable.
    C. Not very valuable.
    D. I have not reviewed the marketing slides yet.
    E. Other: please explain on the comment page at the back of this handout.

COMMENTS

Write out any additional comments about specific courses or the plenary session (please indicate which), and list suggestions for topics and speakers for future meetings. Leave at the AANEM Registration and Information Center or mail to the AANEM Executive Office at 2621 Superior Drive NW, Rochester, MN 55901.